



UPPSALA
UNIVERSITET

*Digital Comprehensive Summaries of Uppsala Dissertations
from the Faculty of Medicine 1927*

One-click away from higher contrast

*Improvements to peripheral clearance for same-day
immunoPET in Alzheimer's disease*

EVA SCHLEIN



ACTA
UNIVERSITATIS
UPSALIENSIS
UPPSALA
2023

ISSN 1651-6206
ISBN 978-91-513-1765-6
URN urn:nbn:se:uu:diva-499059

Dissertation presented at Uppsala University to be publicly examined in Rudbecksalen, Dag Hammarskjölds Väg 20, Uppsala, Friday, 12 May 2023 at 09:15 for the degree of Doctor of Philosophy (Faculty of Medicine). The examination will be conducted in English. Faculty examiner: PhD Jordi Llop Roig (Radiochemistry and Nuclear Imaging Department).

Abstract

Schlein, E. 2023. One-click away from higher contrast. Improvements to peripheral clearance for same-day immunoPET in Alzheimer's disease. *Digital Comprehensive Summaries of Uppsala Dissertations from the Faculty of Medicine 1927*. 76 pp. Uppsala: Acta Universitatis Upsaliensis. ISBN 978-91-513-1765-6.

The brain is a challenging target for antibody-based positron emission tomography (immunoPET) to image amyloid-beta (A β). Antibodies detect pathology with high sensitivity, but due to their size and biological half-life, they cause a high background radiation, if radiolabelled. Antibodies fused to transferrin-receptor (TfR) binders can penetrate the BBB via receptor-mediated transcytosis.

In this thesis, I evaluated several methods to reduce the biological half-life for bispecific antibodies, which bind to A β and TfR, to reduce the time between injection and imaging.

In paper I, we studied two different clearing approaches – direct clearance and induced clearance – to reduce blood concentrations of a monospecific and a bispecific, brain penetrating antibody, for enhanced contrast. The direct clearing approach was too efficient to show a benefit for brain imaging. The induced clearing strategy, based on the inverse-electron demand Diels–Alder (IEDDA) reaction of a TCO and a tetrazine, proved the concept of induced clearance for the monospecific antibody, but not for the bispecific antibody. For paper II, we changed the antibody design and compared a bispecific antibody with its corresponding monospecific variant, both with and without a mutation that attenuated binding to the neonatal Fc receptor (FcRn), to decrease antibody circulation time *in vivo*. The mutation reduced the blood half-life and we suggested an imaging time 12 to 24 h after injection. In paper III, we radiolabelled both FcRn mutated antibody constructs with fluorine-18, to compare their pharmacokinetic profiles in WT mice with PET imaging over 9 h. The bispecific antibody, that showed higher brain uptake, was then injected into WT and AD mice (App^{NL-G-F}). PET scanning 12 h after injection revealed higher antibody retention in App^{NL-G-F} compared to WT mice. In paper IV, we tested two novel tetrazines for their potential to be used as pre-targeting agents. Pre-targeting describes a two-step approach with the aim to achieve a high contrast PET image. First a TCO-modified antibody is injected and after a while a second substance, a radiolabelled tetrazine is injected. Successful pre-targeting requires a tetrazine which can penetrate the brain and then be efficiently cleared. We could show that both fluorine-18 labelled tetrazines entered the brain, where one of them was more efficient than the other.

In conclusion we have shown that it is possible to increase the peripheral clearance of radiolabelled antibodies and get one step closer to same-day immunoPET imaging.

Keywords: Alzheimer's disease (AD), bispecific antibody, Amyloid- β (A β), Receptor mediated transcytosis (RMT), Neonatal Fc receptor (FcRn), Blood-brain barrier (BBB), Inverse electron demand Diels–Alder reaction IEDDA, pre-targeting, tetrazine, bio-orthogonal, Fluorine-18, clearing agent

Eva Schlein, Department of Public Health and Caring Sciences, Geriatrics, Box 609, Uppsala University, SE-75125 Uppsala, Sweden.

© Eva Schlein 2023

ISSN 1651-6206

ISBN 978-91-513-1765-6

URN urn:nbn:se:uu:diva-499059 (<http://urn.kb.se/resolve?urn=urn:nbn:se:uu:diva-499059>)

Nothing in life is to be feared, it is only to be understood – Marie Curie

List of Papers

This thesis is based on the following papers, which are referred to in the text by their Roman numerals.

- I. **Schlein, E.**, Syvänen, S., Rokka, J., Gustavsson, T., Rossin, R., Robillard, M., Eriksson J., Sehlin D. (2022) Functionalization of Radiolabeled Antibodies to Enhance Peripheral Clearance for High Contrast Brain Imaging. *Mol Pharm.*, 19(11), 4111-4122
- II. **Schlein, E.**, Andersson, K. G., Dallas, T., Syvänen, S., Sehlin, D. Reduced Neonatal Fc Receptor Binding Increases Clearance and Brain-to-Blood Ratio of a Brain Penetrating Amyloid- β Antibody. *Manuscript*
- III. **Schlein, E.**, van den Broek S., Dallas, T., Andersson, K. G., Syvänen, S., Eriksson J., Sehlin, D. A β targeting ImmunoPET: Brain pharmacokinetic comparison between a brain penetrating and a regular antibody. *Manuscript*
- IV. **Schlein, E.**, Rokka, J., Odell, L. R., van den Broek S., Herth M. M., Battisti U. M., Syvänen S., Sehlin, D., Eriksson J. Synthesis and Evaluation of Fluorine-18 labelled Tetrazines as Pre-targeting Imaging Agents for PET. *Manuscript*

Additional Publications

Publications not included as part of this thesis:

- V. Rokka, J., **Schlein, E.**, Eriksson J. (2019) Improved synthesis of SV2A targeting radiotracer [¹¹C]UCB-J. EJNMMI Radiopharm Chem. 4(1):30
- VI. Xiong, M., Roshanbin, S., Rokka, J., **Schlein, E.**, Ingelsson, M., Sehlin, D., Eriksson, J., Syvänen, S. (2021) Neuroimage 239:118302
- VII. Syvänen, S., Meier, S., Roshanbin, S., Xiong, M., Faresjö, R., Gustavsson, T., Bonvicini, G., **Schlein, E.**, Aguilar, X., Julku, U., Eriksson, J., Sehlin, D. (2022) Pharm Res. 39(7):1481-1496

Contents

Additional Publications.....	6
Introduction.....	13
Alzheimer's disease.....	13
Amyloid-beta and the amyloid cascade hypothesis.....	13
A β targeted therapy.....	15
Fluid Biomarkers.....	16
Amyloid PET Imaging in AD.....	17
ImmunoPET imaging of A β	18
Drug delivery over the Blood Brain Barrier.....	19
Recombinant antibody engineering.....	20
Radionuclides.....	24
Iodine-124 and Iodine-125.....	24
Fluorine-18.....	25
Radiometals.....	26
Bio-orthogonal reactions for brain-imaging.....	26
Methodology.....	28
Mouse models.....	28
Recombinant protein-expression.....	28
Antibody modifications.....	29
Mannose.....	29
TCO-Modification.....	30
Clearing Agent.....	30
Verification of TCO-modification.....	30
Radiochemistry.....	31
Iodine labelling.....	32
Binding assays.....	32
ELISA.....	32
Surface plasmon resonance (SPR).....	32
FcRn Column.....	33
Imaging.....	33
PET and SPECT.....	33
Brain distribution of radiolabelled antibodies.....	34
Immunostaining.....	34
Autoradiography.....	34

Nuclear track emulsion	35
Aims	36
Summary of Paper I-IV	37
Paper I	37
Paper II	38
Paper III	39
Paper IV	40
Results and discussion	42
Increased peripheral clearance	42
Reverse Gatekeeping – you shall not leave?	44
One click to success?	45
Considerations for the design of brain immunoPET ligands	47
Conclusion and future perspective	49
Popular Science Summary	51
Populärwissenschaftliche Zusammenfassung	53
Funding	55
Acknowledgments	56
References	59

Abbreviations

^{11}C	Carbon-11
^{125}I	Iodine-125
^{18}F	Fluorine-18
AD	Alzheimer's disease
ADCC	antibody-dependent, cell-mediated cytotoxicity
APP	Amyloid precursor protein
Arc	Arctic mutation
ARIA	amyloid-related imaging abnormalities
ARIA-E	ARIA-edema
A β	Amyloid beta
A β PF	A β protofibril
A β PP	A β precursor protein
BACE1	β -site APP cleaving enzyme 1
BBB	Blood-brain barrier
BD-tau	brain-derived tau
CA	clearing agent
CCO	<i>cis</i> -cyclooctene
CDC	complement-dependent cytotoxicity
CH	constant heavy
CL	constant light
CNS	Central nervous system
CSF	Cerebrospinal fluid
CT	computed tomography
DFO	deferoxamine
DOTA	1,4,7,10-tetraazacyclododecane-1,4,7,10-tetraacetic acid
DTPA	diethylenetriaminepentaacetic acid
ELISA	Enzyme-linked immunosorbent assay
Fab	Fragment antigen binding
FBA	Fluorobenzaldehyde
Fc	Fragment crystallisable
FcRn	Neonatal Fc-receptor

FDG	2-[¹⁸ F]Fluoro-2-deoxy-D-glucose
Fv	Fragment variable
HCAbs	camelid derived heavy chain antibodies
HRP	Horseshoe peroxidase
HTz	H-Tetrazine
ID	Injected dose
IEDDA	Inverse-electron-demand Diels–Alder
IgG	Immunoglobulin G
IgNARs	Immunoglobulin new antigen receptors
IMGT	international ImMunoGeneTics information system®
ISF	Interstitial fluid
kDa	kilo Dalton
mAb	Monoclonal antibody
MeTz	methyl-tetrazine
MRI	Magnetic resonance imaging
NOTA	1,4,7-triazacyclononane-1,4,7-triacetic acid
NTE	Nuclear track emulsion
PBS	Phosphate buffered saline
PET	Positron emission tomography
PiB	Pittsburgh compound B
p-tau	Phosphorylated tau
RAGE	receptor for advanced glycation end products
RMT	Receptor mediated transcytosis
sAPPβ	soluble APP fragment
scFv	Single-chain variable fragment
SCN	Isothiocyanates
sdAb	Single domain antibody
SDS-PAGE	Sodium dodecyl sulfate polyacrylamide gel electrophoresis
SFB	N-Succinimidyl-4-[¹⁸ F]-fluorobenzoate
SPECT	single-photon emission computed tomography
SPR	Surface Plasmon Resonance
SUV	Standard uptake volume
Swe	Swedish mutation
TCO	Trans-cyclooctene
TfR	Transferrin receptor
tg	Transgenic
t-tau	total tau
VH	variable heavy
VHH	Variable heavy chain domain

VL	variable light
VNAR	variable domain of new antigen receptor
WT	Wild type

Introduction

Alzheimer's disease

Old age is characterised by an array of age-related conditions, including Alzheimer's disease (AD). Symptoms of AD include decline with speech or language, difficulty performing spatial tasks, obsessive or impulsive behaviour, memory impairment and other diminishing in domains of cognition. Before any symptoms of AD arise, pathological processes in the brain start and the slow progression of neurodegeneration begins.^{1,2} As the name indicates, neurodegenerative diseases describe a group of conditions in which the damage or loss of neural function is a key process, causing an impairment of brain functions such as learning, memory and orientation. Dementia is an umbrella term for a condition caused by different diseases, of which AD is the most common one.¹

Genetic mutations are responsible for up to 1%³ of early onset AD cases and the majority of AD cases are called sporadic AD. Neuropathological hallmarks of AD are extracellular dense core plaques consisting of amyloid-beta ($A\beta$) and neurofibrillary tangles which are composed of aggregated tau protein.² Pathological changes, such as $A\beta$ aggregation, followed by tau aggregation, atrophy of the brain and clinical decline can be observed 15-20 years before clinical symptoms of AD arise. These processes seem to plateau shortly after clinical onset.^{4,5} Biomarkers, to detect these early changes, as well as therapy options, which stop or slow the disease progression are needed.

Amyloid-beta and the amyloid cascade hypothesis

$A\beta$ is a proteolytic cleavage product of the amyloid precursor protein (APP). APP is expressed throughout the body in three isoforms, where the shortest variant (695 isoform) is expressed in the brain by neurons and astrocytes.⁶ To produce $A\beta$, APP is processed by enzymatic cleavage in two steps. First, β -secretase cleaves off the N-terminal domain of APP, resulting in the release of a soluble APP fragment (sAPP β). The remaining C-terminal APP fragment is then further processed by γ -secretase. As a result of different γ -secretase cleavage sites on APP, $A\beta$ peptides ranging from 38 to 43 amino acids are produced. The most common forms of $A\beta$ peptides are 40 and 42 amino acids in lengths, where $A\beta$ 40 is 10-times more produced in the brain.^{7,8} $A\beta$ 42 contains 2 more amino acids at the C-terminus that influence its hydrophobicity

and therefore its propensity to aggregate and to accumulate in the brain tissue.⁸ The aggregation of A β is believed to start with misfolding of the protein, which starts to aggregate into soluble oligomers and protofibrils, which eventually form insoluble A β fibrils that finally deposit in the form of plaques (Fig. 1). Soluble A β 42 aggregates are associated with early forms of pathology in AD⁹ and are thought to induce a cascade of downstream events that eventually lead to AD, as postulated by the amyloid cascade hypothesis. This hypothesis was initially proposed in 1992¹⁰ and it pinpoints the accumulation of A β as the main cause of the disease.^{11,12} This initiates hyperphosphorylation, aggregation and accumulation of the tau protein, which in turn leads to synaptic failure, neurodegeneration and brain atrophy. All these events are accompanied by inflammation, which overall occurs by activation of the immune system in the brain, more specifically microglia and astrocytes. These glial cells try to remove the toxic proteins as well as dying cells, which establishes a chronic inflammation. Due to cell loss, the brain shrinks and shows a decreased ability to metabolise glucose which eventually results in compromised brain functions.¹

A number of physiological functions of A β have been proposed, such as synaptic regulation and memory formation in hippocampus, as well as facilitation of neuronal growth and survival. It has been observed that A β is prone to an effect called hormesis, which means that at low (physiological) concentrations the afore mentioned processes could get enhanced, whereas at high (pathological) concentrations these processes get inhibited.^{13–19} Further, A β has been suggested to be involved in repairing leaks in brain vasculature²⁰ as well as being protective against oxidative stress, toxins and pathogens,^{21,22} the latter through a specific protective antimicrobial effect²³.

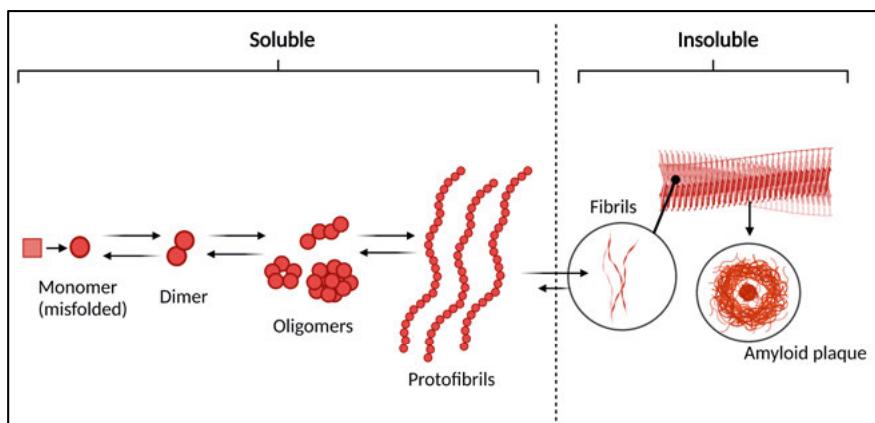


Figure 1. Aggregation of A β . Adapted from Rebecca Faresjö Melander's thesis (2023)

A β targeted therapy

Since the proposal of the amyloid cascade hypothesis, an obvious aim for AD therapy has been to reduce the A β burden in the brain. Different targets have been explored so far, such as decreasing the β - or γ -secretase pathways to suppress A β production and accumulation, or by increasing the clearance of already existing A β deposits.²⁴ Each of these targets has led to a number of developed treatment strategies. The β -secretase pathway is mediated by the β -site APP cleaving enzyme 1 (BACE1) and has been the target for several clinical trials with small molecules²⁴. It has also been explored in our group.²⁵ After several failures, clinical trials on BACE1 inhibitors were stopped.²⁶ Another target for drug development was the receptor for advanced glycation end products (RAGE), a cell surface receptor, which is linked to increased A β plaque formation.²⁷ This receptor has been shown to cause inflammation in the brain and was hypothesized to increase A β clearance when blocked.²⁷ But the clinical trials for the RAGE antagonist have been stopped as phase 3 clinical trials did not meet the primary endpoints.²⁸

Not just small molecules, but also antibodies for A β clearance were explored in clinical trials. Initially, many trials failed²⁴ and this has sparked discussions on the optimal aggregation state of A β for therapy, where different target strategies have been explored.²⁹ Three antibodies which were developed for AD therapy will be further described due to their current importance for drug development and relevance for this thesis. Two of these have been conditionally approved by the FDA and increased the hope for future therapy.^{30,31} This is the first time since the discovery of AD that a disease modifying treatment may be offered to patients.

Bapineuzumab

Bapineuzumab is a humanised IgG1 antibody, based on the mouse antibody 3D6 that binds with high affinity to the N-terminus of A β (amino acid 1-5). This epitope is available in all aggregation forms of A β and it thus binds to both soluble and fibrillar A β of different structures. This antibody was the first monoclonal antibody to enter human testing in clinical trials. In a 12-month phase 1 clinical trial, a subset of treated patients showed abnormalities, visualized with MRI imaging, that were identified as microhemorrhages. These microhemorrhages occurred in patients which received the highest dose of 5 mg/kg. Due to these findings, the Alzheimer's Association Research Roundtable coined the term amyloid-related imaging abnormalities (ARIA) – more specifically ARIA-edema (ARIA-E) for vasogenic edema and ARIA-H to describe microhemorrhages.³² The clinical trials to explore the possibility of bapineuzumab as therapeutic medication were stopped in 2012 due to insufficient therapeutic effect. Clinical data revealed no effect of bapineuzumab to protect patients participating in the trials from cognitive and functional decline, despite positive biomarker results.³³

Lecanemab

Lecanemab is the humanised IgG1 version of the mouse monoclonal antibody mAb158 that binds selectively to large, soluble A β protofibrils at the N-terminus of A β (amino acids 1-16).³⁴ It binds selectively to A β aggregates via avidity.³⁵ As figure 2 describes, affinity refers to the strength of a single interaction between antibody and antigen. Avidity however describes the total strength of all non-covalent interactions, meaning for example the combined binding with both arms of an IgG antibody. Thus, mAb158 binds with low affinity to A β monomers, but with high avidity to A β aggregates, which contain multiple monomeric units.

In 2019, a Phase 3 clinical trial was started and by October 2022, positive top-line results were reported. After 18 months of treatment, the antibody had slowed down the cognitive decline by 27%. In addition, two-thirds of the treated group became amyloid-PET negative within 18-months and had an overall positive outcome on biomarkers with few ARIA side-effects.³⁶ This antibody was recently granted a conditional FDA approval³⁰ and will be marketed by the name Leqembi®.

Aducanumab

Aducanumab is a human IgG1 antibody which is targeted against A β aggregates and binds to the N-terminus of A β (amino acids 3-7).^{34,37} In 2021, the FDA conditionally approved this antibody,³¹ causing a controversial response amongst the scientific community.^{38,39} The controversy included doubts regarding the benefits versus the risks of the treatment, more specifically regarding ARIA side-effects, especially considering the modest impact the treatment had on cognition.⁴⁰⁻⁴³ The antibody will be marketed by the name Aduhelm®.

Even though antibodies with their high target specificity are extremely attractive for therapy, there have been concerns regarding the economic costs.⁴⁴

Fluid Biomarkers

Fluid biomarkers are currently used in AD diagnosis, especially markers measured in Cerebrospinal fluid (CSF), which are sampled via lumbar puncture. The CSF is a protective liquid which is surrounding the entire brain and responsible for clearing waste products. Due to its close proximity and connection to the brain, CSF partly reflects the biochemical environment of the brain.^{45,46}

The clinically used CSF markers for AD diagnosis are A β 42 or a ratio of A β 42/A β 40, as well as total tau (t-tau) and phosphorylated tau (p-tau). In

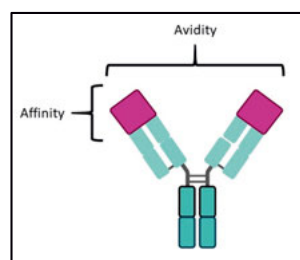


Figure 2. Difference between affinity and avidity.

patients with AD, the accumulation of A β 42 in the brain increases, which causes the soluble A β 42 in CSF samples to decrease. However, the A β 42/40 ratio has a better prediction value for pathological changes within the brain than each value on its own, as it takes into account the naturally occurring variation in A β production.^{47,48}

T-tau can be used to evaluate general neurodegeneration, as it is not just elevated in AD but also increased in traumatic brain injury and other dementias.^{49,50} The elevated level of p-tau in CSF samples, is an indication of neuronal damage and pathological tau phosphorylation in the brain.⁵¹

CSF sampling is considered to be invasive. Blood biomarkers are more accessible, and therefore less expensive. New techniques are emerging to detect soluble A β oligomers and to predict AD with high accuracy and sensitivity.⁵² Further, p-tau markers such as p-tau181, p-tau217 and p-tau231 show great diagnostic potential in differentiating AD from other neurodegenerative diseases. Interestingly, they seem to closer reflect the brain's A β pathology rather than the tau pathology.⁵³⁻⁵⁹ This year a new tau blood maker was published, which shows potential to differentiate AD from non-AD. This new biomarker is called brain-derived tau (BD-tau) and represents an immunoassay which was developed using a monoclonal antibody (TauJ.5H3) which selectively binds CNS tau isoforms.⁶⁰

Fluid biomarkers are an important tool for cost efficient diagnosis of AD. However, as they are collected in the periphery, they can only serve as a proxy of processes that occur inside the brain. In this respect, PET imaging can give better insight about the spatial distribution of the pathology and thereby about the disease processes in the brain.

Amyloid PET Imaging in AD

In order to understand and prevent the progression of neurodegeneration, visualising the processes in the brain is crucial. A big breakthrough in the field of A β imaging was the introduction of the small molecule PET-tracer carbon-11-labelled Pittsburgh Compound B ([¹¹C]PIB). [¹¹C]PIB is a thioflavin-T derivative that binds to the beta-sheet of insoluble amyloid fibrils, and it was the first PET amyloid tracer developed to image A β deposits in AD patients.^{61,62} [¹¹C]PIB is labelled with carbon-11, which has a half-life of 20 min. The short half-life makes it necessary for the production facility to be on-site and limits therefore its distribution. Second generation amyloid tracers were developed using fluorine-18 as radioisotope. This isotope has a half-life of 110 min, which facilitated the possibility to transport the tracer from the production site to scanner sites. Three fluorine-18 labelled tracers, Flortbetapir, Flutemetamol and Flortbetaben are approved by the FDA.⁶³ These imaging tracers have given valuable information about A β pathology and have been extensively used for AD therapy clinical trials.

A drawback of current amyloid tracers is the exclusive binding to the dense amyloid core of insoluble A β plaques. Amyloid deposition displays a plateau around the time of clinical disease onset and may therefore not accurately depict the entire proceedings of the disease.^{64–66} Further, soluble and diffuse A β -aggregates, such as oligomers and protofibrillar A β , that are seen as more toxic, are not monitored with these tracers.^{64,67}

ImmunoPET imaging of A β

Antibodies are a class of molecules which is characterised by their high affinity and specificity for their respective target. PET imaging with antibody-based tracers, immunoPET, has been shown to have certain advantages in spatial resolution, image quality and quantification.⁶⁸ The concept to use antibodies for imaging purposes is more than two decades old,⁶⁹ but was explored mainly for cancer imaging so far. An immunoPET ligand which can bind all forms of A β would be attractive as it could be used to follow the changes during the whole development of A β pathology in AD. As nonfibrillar A β oligomers and protofibrils have been observed to have a dynamic profile during disease progression, they could be a better imaging target than amyloid plaques. Due to the specific binding to their target, antibody-based imaging ligands could thus be more suitable than small molecules like [¹¹C]PIB for imaging of dynamic processes such as disease progression and the effects of therapy. In our group we have developed a number of antibody tracers which target A β aggregates in AD mouse and rat models.^{70–74} We have also compared the performance of an iodine-124 labelled antibody-based tracer with [¹¹C]PIB. [¹¹C]PIB failed to display A β pathology devoid of dense-core plaques, which made it less dynamic than the antibody ligand in terms of detecting different stages of disease progression.⁷¹ In addition, while the antibody detected effects of A β lowering treatment both at an early⁷⁵ and late²⁵ stage of A β pathology, [¹¹C]PIB could not detect the effects of treatment in either of two mouse models of A β pathology.⁷⁶ Moreover, antibody-based PET corresponds well with *ex vivo* analysis of AD mice brain pathology.⁷⁵

An important advantage of immunoPET is target specificity and as an antibody can in principle be produced against any protein antigen, the variety of potential targets is unlimited. Thus, there is a potential for further development in regards of new targets, including for example neuroinflammation targets such as TREM2⁷⁷ and GFAP⁷⁸, or other protein aggregates such as alpha-synuclein.⁷⁹

But challenges in the immunoPET development of antibody-based tracer remain. The long blood half-life of antibody based tracer requires the use of radioisotopes with matching half-lives, which would cause issues regarding logistical planning for clinical applications. The radiation exposure for the patient would be high and the hospitals would have to isolate the patient, to limit

the exposure to personnel. A short time between injection and image acquisition are preferred in clinics as it allows the use of radioligands radiolabelled with fluorine-18, which gives high resolution images and, due to its short half-life, minimizes the exposure of the patient. An additional challenge in development of immunoPET tracers for brain targets is the blood-brain barrier (BBB), which is an obstacle in delivery of drugs to the brain, especially large molecules such as proteins.

Drug delivery over the Blood Brain Barrier

The brain is the centre of the human being and due to its importance a highly protected organ. The interstitial fluid (ISF) of the brain and the blood plasma show distinctly different compositions, which is why the BBB is of great importance for the stability of the brain microenvironment. It is composed of a continuous endothelium without fenestrations, enabling it to act like a selective barrier that prevents substances in the blood from reaching the central nervous system (CNS). Pinocytotic vesicles are not very densely distributed in its endothelium, which is indicating that this barrier is not as permeable, as other organ endothelia. Beyond this, surrounding astrocytes and pericytes support and regulate the BBB, helping to maintain it.⁸⁰⁻⁸² The paracellular flux of ions and hydrophilic solutes through the BBB is restricted by the inter-endothelial transmembrane tight junction proteins. This results in a high electrical resistance and explains the low permeability of polar molecules.⁸³⁻⁸⁵

Despite the restricted access, the BBB allows lipophilic and hydrophilic substances the transport over the barrier via passive (diffusion) or active transport. There are five different possible ways of a substance to enter the brain across the BBB:

1. Simple diffusion
2. Facilitated diffusion
3. Active transport
4. Adsorptive transcytosis
5. Receptor mediated transcytosis⁸⁰

Due to their size of >150 kDa, antibodies usually do not pass the BBB, and their brain concentration has been reported to be about 0.1% of their serum concentration.⁸⁶ When normalised to the weight of the brain, our lab could show concentrations of 0.03-0.14%ID/g of radiolabelled antibody in the brain of a mouse.^{70,87-89} To overcome the issue of low brain delivery, the IgG based antibodies can be modified to get transported into the brain via receptor mediated transcytosis.⁹⁰ The transferrin receptor (TfR) has been intensively studied for this purpose.^{91,92} Referred to as “molecular Trojan horse”, this method could increase the concentration of a bispecific antibody, which consists of an

IgG base conjugated to single-chain variable fragments (scFv) of an anti-mouse TfR antibody, called 8D3, up to 80-fold higher, compared to non-modified antibody.⁷⁰ The name “Trojan horse” was chosen, to emphasize the alternative use of the transferrin receptor, as the physiological role of TfR is the transport of iron over the BBB into the brain.⁹³

TfR mediated transcytosis has been widely used in preclinical studies of drug delivery and several key factors have been identified for successful design of a BBB crossing antibody. The antibody should not interfere with the innate function of the TfR, which is why many antibodies which bind the TfR are designed to bind the apical domain of the receptor.^{91,94-97} Further, the affinity to the TfR plays a crucial role in the efficiency of brain delivery. A nanomolar range (50-100 nM⁹⁸ or 6-10 nM⁹⁹) has been proposed as optimal TfR affinity. A monovalent interaction is preferred over a bivalent interaction, as the bivalent interaction could lead to a clustering of TfR on the cell surface and eventually lysosomal degradation.^{96,100-102} Higher affinity binders might be trapped in the blood vessels and sorted into lysosomes for degradation, induced by receptor clustering.^{96,103,104} but if the TfR affinity is too low, the brain delivery will be insufficient.¹⁰⁵ The injected dose also has to be considered, as tracer dosing requires higher affinity binders to increase the uptake⁹⁸, whereas at high doses, low affinity binders are better suited to achieve high brain uptake.⁹⁸ The pH plays a crucial influence as well, as antibodies bind to the TfR at physiological pH, but dissociate from the receptor at lowered pH.^{98,106} Another important influence is the way the antibody binds, its valency. All in all, the design of the bispecific antibody matters.

Our group could design various constructs of antibodies which are capable of passing the BBB, by linking a transferrin receptor (TfR) binding antibody 8D3 to antibodies against A β for receptor mediated transcytosis^{70,71,73,107,108} an increased uptake in the brain could be observed.¹⁰⁹

Recombinant antibody engineering

Since the introduction of the hybridoma technology in the 1970s, the production of monoclonal antibodies became easier and fundamental improvements in protein research could be achieved.¹¹⁰

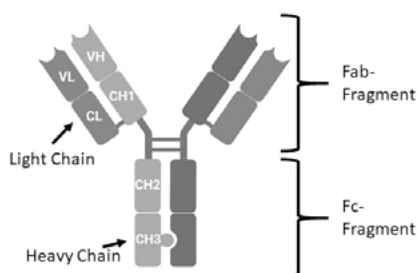


Figure 3. General structure of IgG antibody. Here the knobs-into-hole design is displayed.

Antibodies are used in various ways, one of which is imaging. Generally therapeutic antibodies belong to the Immunoglobulin G (IgG) isotype. This isotype is the most abundant in human serum. Four subclasses have been reported which differ in their hinge and C_{H2} domain. Antibodies are comprised of four polypeptide chains; two identical heavy chains and two light chains, with an overall molecular weight of around 150 kDa. The heavy and light chains are connected via disulphide bonds and consist of constant (constant heavy - CH and constant light - CL) and variable domains (variable heavy - VH and variable light - VL, Fig. 3). The target specific binding region of an antibody is consisting of the variable domain of heavy and light chain, and together with the C_{H1} domain they form the Fab region. The fragment crystallisable (Fc) region is composed of the C_{H2} and C_{H3} and has several functions, such as extending the circulation time *in vivo*, as well as binding to immune cells to induce phagocytosis or activation of immune processes, so called effector functions.¹¹¹

The high specificity of the antibodies to their antigen makes them a promising tool for targeted *in vivo* radio imaging. With protein engineering many different antibody formats can be achieved. Besides conventional IgGs, formats based on antibody fragments can be generated either by enzymatic digestion, to obtain e.g. F(ab')₂ and Fab fragments, or by recombinant design and expression, resulting in e.g. single-chain variable fragments (scFv), single domain antibodies (sdAb), diabodies etc.¹¹² All of these antibody constructs come with their own set of advantages and challenges in the context of radio imaging applications. Full-length IgGs and larger antibody fragments exceed the glomerular filtration cut off (60 kDa) and increase the radiation-burden on the liver due to the hepatic clearing route. Further as the neonatal Fc receptor increases the serum half-life, by protecting the antibody from catabolism, the biological half-life of the antibody needs to be matched with long-lived radionuclides.^{113–115} Smaller constructs have been developed to increase the clearance time of unbound tracer from blood and to achieve a higher target to background ratio. Naturally occurring, smaller antibodies are shark derived immunoglobulins (IgNARs)¹¹⁶ or camelid derived heavy chain antibodies (HCAbs).¹¹⁷ The variable domain of these antibodies (VNAR, VHH) can be isolated and used as a single domain antibody, with a molecular weight of 15 kDa and fast pharmacokinetics *in vivo*.¹¹⁸ These small molecules are well

perceived in the cancer imaging field,^{119,120} but have their own set of limitations as well, like high kidney retention, due to their path of clearance^{121,122} or a low accumulation in the target tissue, due to fast blood clearance.¹²³

Bispecific antibodies are of great interest for both therapeutic and diagnostic applications. In general the term bispecific for antibodies means, that an antibody can bind to two different antigens simultaneously.¹²⁴ In our lab we have used different bispecific antibody designs, such as a F(ab')₂ fragment of the humanised version of the A β protofibril selective mAb158, connected to a full 8D3 antibody. As well as a recombinant version of mAb158 where two single chain variable fragments (scFv) of 8D3 were fused to the C-terminus of the light chains. Another design included a tribody consisting of two scFv158 connected to a Fab-8D3 or a scFv3D6 connected to an scFv8D3.¹²⁵ Each of these designs were evaluated for their potential as immunoPET tracers and showed their own set of benefits and challenges. For this thesis we wanted to create a bispecific antibody construct which is based on an IgG, connected to one Fab fragment of 8D3 (Fig. 4). To achieve this goal we used the knobs-into-holes antibody design. This established method utilises the heavy chains of the antibody for heterodimerization. Here a knob variant was obtained by exchanging two small amino acid with big amino acids on the first C_H3, like T366W, where T with an IMGT volume class of 116.1 Å³ is considered small and W with a volume of 227.8 Å³ is considered big.¹²⁶ IMGT is an abbreviation for international ImMuNoGeneTics information system®, which provides standardised data about immunogenetics and immunoinformatics.¹²⁷ For the hole, four large amino acid were exchanged with small amino acids on the second C_H3.¹²⁸ For further stabilisation additional disulphide bridges were implemented.^{129,130}

Besides changing the structure of IgG antibodies to allow heterodimerization, other ways to engineer antibodies can be used to modify their *in vivo* behaviour. We further included a mutation to the knob-into-hole design which is common for therapeutic antibodies. The Fc region of antibodies has several effector functions. For an imaging agent, which is circulating in an organism for several days, silenced effector functions are desirable. This can be achieved by eliminating binding to the Fc- γ receptor in through introduction of the following mutations to the IgG Fc region: L234A, L235A, P329G (LALA-PG). IgG1 type antibodies have a high level of innate cytotoxic functions, which causes an immune response via two different pathways.¹³¹ Either the complement-dependent cytotoxicity (CDC) or the antibody-dependent, cell-mediated cytotoxicity (ADCC). The CDC initiates an immune response where protein components of the serum attack pathogens via the activation of a biochemical cascade.¹³² During the ADCC response an effector cell of the immune system lyses the cell the antibody is bound to.^{133,134} The mutation L234A and L235A have been shown to effectively reduce the ADCC re-

sponse, as they are important for the Fc- γ receptor binding on the C_H2 domain.¹³⁵ The P239A mutation has in addition been shown to effectively reduce the CDC activity, without disturbing the ADCC activity.¹³⁶

Besides being important for effector functions, the Fc domain also plays an important role for the serum half-life of antibodies.¹³⁷ Binding to the neonatal Fc receptor (FcRn) is believed to recirculate an antibody and to extend its biological half-life.¹³⁸ By mutating the binding region for the FcRn on the Fc-domain of the antibody, H310A/H435Q (HAHQ), a reduced blood half-life could be shown, but has to our knowledge not yet been applied to neuroimaging.^{139–143}

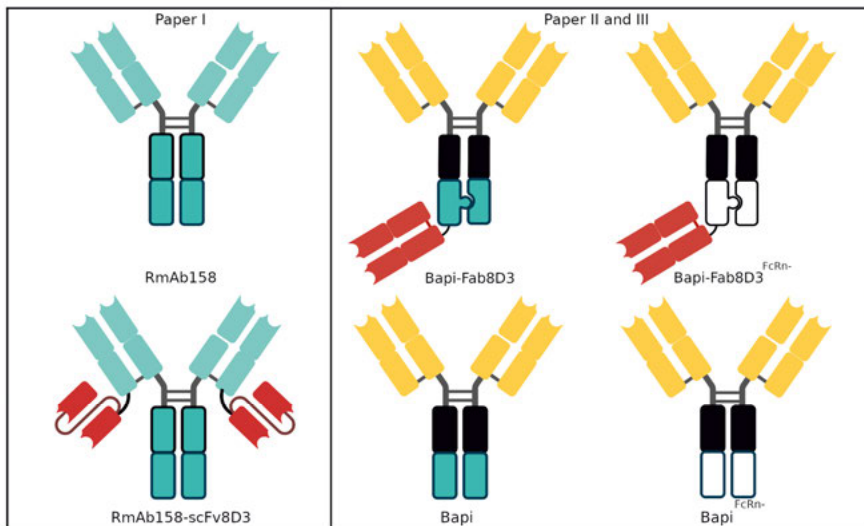
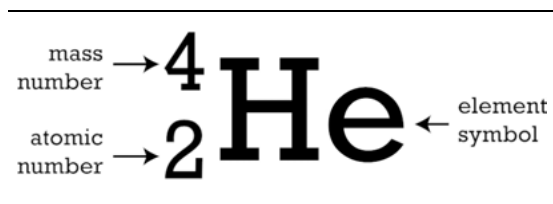


Figure 4. Structure of antibodies which were used in this thesis. In paper I we used RmAb 158 in a monospecific or bispecific format with single chain variable fragments of 8D3. For paper II and III we used Bapineuzumab with two different designs. A monospecific, bispecific design, which was created by using the knob-into-hole design to containing a Fab8D3. All antibodies included LALA-PG mutations (indicated as black box in Fc region), and two constructs contained the HAHQ mutation (indicated as white box in Fc region).

Radionuclides



An atom is composed of a nucleus at the centre and one or several electrons orbiting around it, according to Bohr's atomic theory. Primarily the nucleus is built from protons and neutrons - all together called nucleons.

Figure 5. Atomic number.

By definition an atom consists of an equal number of protons in the nucleus as number of electrons orbiting, giving a balanced charge. The chemical properties of an element is determined by the electronic configuration, whilst the nuclear arrangement defines the stability and radioactive decay of the nucleus. In the context of radiochemistry, the term nuclide is important.

The mass number A , atomic number Z and the arrangement of nucleons identify the species of nuclides (Fig. 5). Especially the term isotope is of importance, as it describes nuclides of the same atomic number, with the same chemical properties, but with different mass number (by different number of neutrons).¹⁴⁴ For this work, an important example of a radioactive isotope of fluorine is fluorine-18, as well as of Iodine is iodine-125.

Radioactive isotopes are instable due to their uneven number of neutrons and protons. Because of that they undergo radioactive decay. Several different types of decay are possible, but for this thesis the positron (β^+) decay is of importance to know. A radionuclide, which is positron rich decays via positron emission, accompanied by a neutrino ν . The emitted positron reacts with an electron in its surrounding. This process is called annihilation and emits two photons with an energy of 511 keV. These photons are detected by the PET-camera.¹⁴⁵

Iodine-124 and Iodine-125

In our lab we primarily use two iodine isotopes for our studies, iodine-124 and iodine-125.

Iodine-124 has a half-life of 4.18 days and is produced in a reactor via the ${}^{124}\text{Te}(p,n){}^{124}\text{I}$ reaction, which is one of eight different production paths.^{112,146,147} Iodine-124 became of interest for antibody labelling since imaging with an iodine-124-labelled HMFGE antibody could be demonstrated in 1991.¹⁴⁸⁻¹⁵¹ This radionuclide is attractive for immunoPET as its half-life matches with the biological half-life of antibodies. It decays to tellurium-124 by emitting 23% beta+-emissions with a mean positron energy of 2138 and 819 keV. But during the decay of iodine-124, gamma-rays occur as well, where 50% of these have an energy of 603 keV, causing a background activity

on PET-images, as they cannot be distinguished from 511 keV annihilation photons by the PET-scanner.¹⁵²

A drawback for iodine-124 usage is that it is not feasible to be used for detecting primary thyroid cancers, stomach cancers, and urinary malignancies (e.g., bladder cancer and prostate cancer) as the thyroid and the stomach can scavenge iodide produced by deiodination. Further, this non-residualizing radioisotope is cleared via the urinary tract.¹⁵³

Iodine-125 is produced in a nuclear reactor via neutron capture, $^{124}\text{Xe}(n,\gamma)^{125}\text{Xe} \rightarrow ^{125}\text{I}$. As the name indicates, a target nuclide captures a neutron and the resulting excited nucleus releases energy as gamma-rays. Iodine-125 has a half-life of ca. 60 days. It decays to 100% via electron capture to a metastable state of tellerium-125 and finally to a stable form of tellerium-125, emitting a 35 keV gamma-ray (7%). The radionuclide can be bought commercially in dilute sodium hydroxide solution.¹⁴⁴ Iodine-125 can be used for SPECT imaging and has similar drawbacks regarding the investigation of certain body areas, as iodine-124.

Fluorine-18

Fluorine-18 is a cyclotron produced radionuclide commonly produced with oxygen-18 enriched water, $^{18}\text{O}(p,n)^{18}\text{F}$. The nuclide is recovered as F⁻ from the oxygen-18 water, which can be reused afterwards. The radionuclide has a half-life of ca. 110 minutes, in which the nuclide decays back to oxygen-18 by emitting 97% positron-emission (0.6335 MeV) and 3% electron capture (1.6555 MeV). It often is used to label glucose to produce 2- ^{18}F Fluoro-2-deoxy-D-glucose (FDG). Fluorine-18 is an attractive radionuclide for PET imaging, as it has a short half-life and a low energy positron emission.¹⁴⁴ The short half-life is practical, as it lowers the amount of time healthy tissue will be exposed to radiation. Due to its low positron energy, fluorine-18 displays an advantageous positron range effect, which describes the distance a positron has to travel within a tissue before annihilation occurs. In other words, the annihilation event takes place close to the position of the radioisotope, resulting in an accurate display of position, which in direct connection creates a high resolution of PET-images.¹⁵⁴⁻¹⁵⁶ Fluorine-18 is suitable for incorporation into organic structures. Several prosthetic groups can be used to be fluorine-18 labelled and bound in a stable way to lysine residues of antibodies, such as N-Succinimidyl-4- ^{18}F -fluorobenzoate (^{18}F SFB)¹⁵⁷ or ^{18}F Fluorobenzaldehyde (^{18}F FBA).¹⁵⁸ In this thesis we labelled tetrazines with fluorine-18 and used the IEDDA reaction to label our antibodies.⁷²

Radiometals

Radiometals have been broadly studied and can be found in clinical applications. They are of interest for antibody labelling due to their straightforward labelling methods, large range of available half-lives and decay properties.¹⁵⁹

Two radiometals which have been explored for molecular imaging of the brain are zirconium-89 and indium-111.^{160,161}

Indium-111

Indium-111 has a half-life of 2.8 days. It can be produced in a cyclotron via $^{111}\text{Cd}(p,n)^{111}\text{In}$ and emits γ -rays which makes it suitable for SPECT imaging.¹⁶² Several chelators can be used for this radiometal, like 1,4,7,10-tetraazacyclododecane-1,4,7,10-tetraacetic acid (DOTA), 1,4,7-triazacyclononane-1,4,7-triacetic acid (NOTA), diethylenetriaminepentaacetic acid (DTPA) and deferoxamine (DFO).¹⁶³ Our lab has experimented with tetrazine-DOTA and a bispecific antibody to explore the use of this radiometal for brain imaging.

Zirconium-89

Zirconium-89 has a half-life of 3.3 days and it decays by positron emission (22.3%) to metastable yttrium-89.¹⁶⁴ It can be produced in several different ways, where the $^{89}\text{Y}(p,n)^{89}\text{Zr}$ and $^{89}\text{Y}(d,2n)^{89}\text{Zr}$ reaction are the most common one.¹⁶⁵ It has been used extensively in the imaging field due to the matching half-life with the circulation time of antibody-constructs.^{166,167} Zirconium-89 can be coupled to antibodies via bifunctional chelators, where a reactive group enables the coupling to lysine or cysteine residues.¹¹² Clinically used chelators are NCS-DFO and DFO-*N*-suc,^{168,169} as well as the recently developed DFO*-NCS.¹⁷⁰ A recent study showed that the choice of chelator is important to image intrabrain targets and DFO*-NCS is preferred over the other explored alternatives.¹⁷¹

Bio-orthogonal reactions for brain-imaging

Conventional IgG antibodies have a size of around 150 kDa and possess a long biological half-life. For them to be used for imaging purposes, the physical half-life of the used radionuclide needs to be matched, forcing the use of long-lived isotopes, such as iodine-124 or zirconium-89.¹²³ However, in clinical practise a long circulation time of a radiolabelled compound is viewed as unreasonable,¹⁷² as it will result in a high dose of activity.¹⁷³ A novel strategy to avoid this issue could be pre-targeting and/or the use of a clearing agent.

The pre-targeting concept can be divided into two steps. In the first step a modified antibody (or any other type of nanomedicine) is injected and is allowed to circulate for a longer period of time to accumulate in the target tissue.

In the second step, a radiolabelled small molecule is injected, interacts with the modified antibody and allows imaging of the target region.¹⁷⁴ The secondary imaging agent should ideally have fast pharmacokinetics and clear from the blood rapidly to provide a high-quality image and a lower radiation burden on healthy tissue.

The concept of pre-targeted imaging or immunotherapy was conceived already in the mid-1980ies, but immunogenic responses were clear drawbacks from the first generation pre-targeting approaches, which changed with the development of bio-orthogonal reactions.^{174–176} Bio-orthogonal reactions are defined as biochemical reactions which do not interfere with the functional groups within the living organism. The term was coined in 2003 and the methodology received a Nobel prize in chemistry in 2022.^{177,178} Several bio-orthogonal reactions exist,¹⁷⁹ but the Inverse-electron-demand Diels–Alder (IEDDA), also called tetrazine ligation, is the most relevant for this thesis. The IEDDA was pioneered by Fox and co-workers, who showed that the reaction between an electron-deficient tetrazine and a highly strained *trans*-cyclooctene (TCO) could take place in complex media like cell lysates.^{180,181} This led to several pre-targeting proof of concepts *in vitro* followed shortly after,¹⁸² as well as *in vivo*,¹⁸³ as well as in the brain.¹⁸⁴

Methodology

Mouse models

Experiments for **paper I** and **paper IV** were conducted using WT mice as well as a transgenic A β pathology model (tg-ArcSwe), both maintained on a C57BL/6 genetic background. Tg-ArcSwe expresses human A β precursor protein (A β PP) with the Swedish (KM670/671NL)¹⁸⁵ and Arctic (E693G)¹⁸⁶ mutations, causing an early onset of A β pathology, starting with intracellular aggregation, followed by parenchymal plaque formation.¹⁸⁷ The plaque formation progresses with age and plaques can be found in cortex, hippocampus, and thalamus, as well as in the cerebellum in later stages. The dense core plaques of tg-ArcSwe are similar to the pathology found in humans.¹⁸⁸

Experiments for **paper II** and **paper III** were performed in WT mice as well as in the human A β PP knock-in mouse model *App*^{NL-G-F}, maintained on a C57BL/6 background. The *App*^{NL-G-F} model carries the Swedish (A β PP KM670/671NL), the Arctic (A β PP E693G) and the Iberian (I716F) A β PP mutations and displays cortical A β deposits already at 2 months of age.¹⁸⁹ In addition to the pathology manifestation of the Arctic and Swedish mutation, the Iberian mutation causes an elevated ratio of A β ₄₂/A β ₄₀. The pathology consists of smaller A β deposits and shows less abundant dense core plaques, as well as an overall diffuse A β -plaque pathology.¹⁹⁰

All procedures described in this study were approved by the Uppsala County Animal Ethics board (C17/14, 5.8.18–13350/2017 and 5.8.18–20401/2020), and were in accord with the rules and regulations of the Swedish Animal Welfare Agency and complied with the European Communities Council Directive of 22 September 2010 (2010/63/EU).

Recombinant protein-expression

In **paper I**, we used the monoclonal antibody mAb158, which binds selectively to A β protofibrils.¹⁹¹ The antibody was expressed in-house, which allowed us to design various antibody variants. Here we have used the recombinant version RmAb158 and attached TfR binders (scFv8D3) to its light chains to obtain the bispecific, brain penetrating version RmAb158-scFv8D3.¹⁹² The antibodies were expressed in Expi293f mammalian cells, transiently transfected with DNA cloned into a plasmid (pcDNA3.4 vectors)

encoding the sequences for the heavy and light chains of the antibody variants and incubated for 7 to 8 days. The antibody was purified from the cell medium with an ÄKTA system, using a protein G column, which binds to the Fc domain of the antibody. The buffer was subsequently exchanged to phosphate buffered saline. Till usage, the proteins were stored at $-80\text{ }^{\circ}\text{C}$.

The antibodies for **paper II** and **paper III** were based on the humanised monoclonal antibody Bapineuzumab and designed with the knob-into-hole technique, based on the Roche brain shuttle format.¹⁹³ A single chain Fab fragment of the TfR antibody 8D3¹⁰⁷ was attached to the C-terminus of the Bapineuzumab heavy chain, this design is based on a reported patent.¹⁹⁴ Additional monovalent Bapineuzumab was produced for comparison reasons. Both antibody formats were designed with and without the inclusion of two mutations: HAHQ, to reduce the binding to the neonatal Fc receptor, and LALA-PG to attenuate effector functions *in vivo*.

The production is described in great detail in **paper II**, in short: the antibodies were expressed recombinantly in ExpiCHO™ cells using the ExpiCHO Expression System Kit. The pcDNA3.4 vectors were added and the transfection was performed according to the manufacturer's instructions. After expression for 7-9 days, the media was harvested by centrifugation. After sterile filtration of the medium, the antibodies were subsequently purified from the cell supernatant with a protein A column using an ÄKTA system. For antibodies without an mTfR binding moiety, the buffer was changed to PBS using a desalting column, subsequent to purification. Bispecific antibodies designed with knobs-into-holes mutations were further purified with size exclusion chromatography (SEC). The peak containing monomeric antibody was collected.

Antibody modifications

For **paper I** antibodies were modified in several different ways to investigate clearance from the body, either directly via mannosylation or with TCO-moieties for induced clearance. To follow the biodistribution of the antibodies *in vivo* the proteins were radiolabelled with iodine-125 for **paper I** and **paper II**. In **paper III** the antibodies were first TCO modified to further be labelled with a fluorine-18 bearing tetrazine.

Mannose

RmAb158-scFv8D3 and RmAb158 were mannolsyated with a D-Mannopyranosylphenyl isothiocyanate. Isothiocyanates (SCN) contain an electrophilic carbon atom, which can react with nucleophiles, such as hydroxyl-, amino-, or thiol-groups (like Tyrosine, Lysine or Cysteine) to form O-thiocarbamates, thiourea or dithiocarbamate. The antibody dissolved in PBS was incubated

with 33 mM sodium carbonate buffer, pH 10, and mannose for 3 h at room temperature. The excess mannose was removed with Zeba spin desalting columns and eluted in PBS.

TCO-Modification

Antibodies designed to interact with the CA or fluorine-18 labelled tetrazines, were modified with *trans*-cyclooctene (TCO). To achieve this modification, the amino-group from lysine residues of the antibody were functionalised with an activated NHS-ester tag attached to the TCO. The antibody, typically 1 mg/ml in PBS was supplemented with 30 mM sodium carbonate buffer, pH 8.0, and reacted with axial TCO NHS dissolved DMSO to 10 mM at a 15-20 x TCO antibody ligand molar ratio. The solution was incubated for 3 h in darkness while shaking at 600 rpm, and subsequently purified from remaining unreacted TCO with a desalting column and eluted in PBS. For experiments with iodine-125, radiolabelling was performed before TCO-modification.

Clearing Agent

Clearing agents (CA) to improve the imaging contrast are being researched on for more than 30 years already, Sinitsyn et al demonstrated the principle of induced clearing by using a (strept)avidin-biotin based clearing agent in 1989 already,¹⁹⁵ and several other methods have been described since then.^{172,176,179,196} A clearing agent we have used in **paper I** was published by Rossin et al. in 2013.¹⁹⁷ This agent is based on albumin and functionalised twice, with a tetrazine-based structure, as well as galactose moieties. The tetrazine will be used for the IEDDA reaction, and the galactose modification is targeting the liver via Ashwell receptors on hepatocytes¹⁹⁶ and thus enhancing the clearance from the blood. Initially designed to enhance the target-to-blood ratio for pre-targeting, we used a clearing agent to remove peripheral radio-labelled antibody to enhance the imaging contrast.

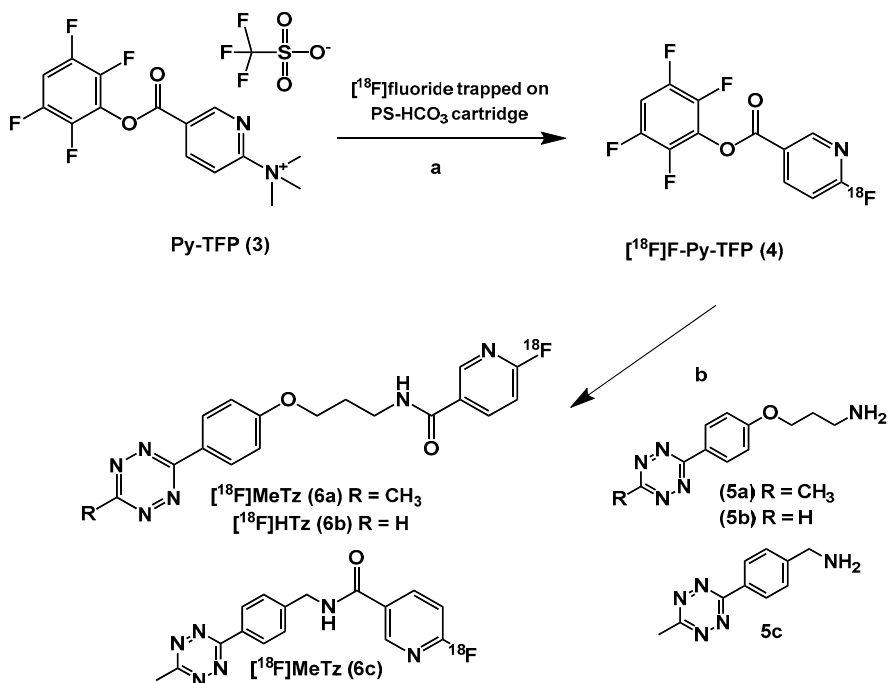
Verification of TCO-modification

In **paper I**, the verification of the TCO modification was done by mixing the TCO modified antibody with the CA (3.0 mg/mL) and incubating it for 30 min while shaking at 600 rpm. Bolt 4x LDS sample buffer was added to the sample and then loaded on a 12 well Bolt 8% Bis-Tris SDS-PAGE gel, which was run at 200 V for 35 min. The gel was exposed to a phosphor imaging plate overnight and after scanning with a Cyclone Plus Imager system at a resolution of 600 dpi, the gel was stained for proteins with PageBlue staining solution. TCO-modification of the antibody could be verified via the size difference of

a negative control and the antibody-TCO-CA mixture. The CA contains albumin and creates in combination with the antibody a higher molecular band on the SDS-PAGE.

Radiochemistry

In **paper III** and **IV**, tetrazines were fluorine-18-labelled with a two-step procedure. [^{18}F]Fluoride was transferred from the cyclotron, trapped on a Chromabond ion-exchange column and reacted on the solid support with a quaternary ammonium precursor passed over the cartridge, omitting the drying of the [^{18}F]fluoride. The effluent containing the formed [^{18}F]Py-TFP prosthetic group was transferred, via a cation exchange cartridge that removed unreacted precursor, to a reaction vessel where the fluorine-18-labelled tetrazines were synthesized by an amidation reaction. Tetrazine **6a** and **6b** were used in **paper IV**, tetrazine **6c** was used in **paper III**.



Scheme 1. [^{18}F]Fluoride was trapped on a Chromabond PS-HCO₃ cartridge and dried with acetonitrile. a) The precursor Py-TFP **3** in acetonitrile was reacted with the [^{18}F]fluoride on the solid support and the formed [^{18}F]F-Py-TFP **4** eluted from the

cartridge . Unreacted precursor Py-TFP **3** was removed by an Oasis MCX Plus cartridge . b) The labelled tetrazines [¹⁸F]MeTz **6a** and [¹⁸F]HTz **6b** [¹⁸F]MeTz **6c** were synthesized by direct amidation.

Iodine labelling

For radioiodination of antibodies, the chloramine T method was used, in which chloramine T oxidizes ¹²⁵I to ¹²⁵I⁺ and the anionic form of tyrosine reacts to ¹²⁵I-tyrosin. To an antibody iodine-125 mixture, chloramine T was added (5 µg, 200 µM in PBS) and incubated for 90 seconds at room temperature. The reaction was quenched by addition of 10 µg (440 µM in PBS) of sodium-metabisulfite. After purifying the radiolabelled antibody with a desalting column, the final activity was measured in an ion chamber. The radiolabelling was performed before the TCO-modification to prevent isomerisation of TCO in to *cis*-cyclooctene (CCO) induced by chloramine T.

Binding assays

ELISA

To estimate antibody binding affinities towards a certain antigen before and after modifications enzyme-linked immunosorbent (ELISA) is a suitable, sensitive and widely used method. This method was used for **paper I to III** as quality control in form of an indirect ELISA or sandwich ELISA. To briefly describe the method: a 96-well plate was coated with Aβ protofibrils, TfR or anti-mouse or anti-human antibody and a sample of modified antibodies were applied in different dilutions. For detection, we used a secondary antibody, conjugated to horseradish peroxidase enzyme (HRP), which was directed towards the Fab region of the primary antibody. HRP reacts with K blue aqueous TMB substrate, the resulted colour change can be detected with a spectrophotometer.

Surface plasmon resonance (SPR)

Developed in the late 1980ies this method can be used as a biosensor for interactions of biomolecules, such as antigen-antibody interactions.¹⁹⁸ For this procedure a protein is immobilised to a dextrane matrix on the sensor surface. An analyte is flushed over the surface in solution and the bound analyte changes the refractive index of the sensor surface, influencing the reflection angle of the lightsource, which can be measured.¹⁹⁹ This is a sensitive method that was used in **paper II** to assess TfR binding of the bispecific antibodies and confirm their monovalent TfR binding.

FcRn Column

First invented to monitor the changes of integrity of the Fc domain of therapeutic antibodies during storage, analysis of the FcRn binding modalities can be used to verify the attenuation of the FcRn mutation as well.²⁰⁰ The FcRn is a non-covalent heterodimer and each interacts with the FcRn binding regions on the Fc domain of the IgG heavy chain in a pH dependent matter.^{201–203} Due to the pH sensitivity of the FcRn binding region of an IgG antibody, the antibody evades degradation by staying bound to the receptor in the acidic environment of endosomes.^{114,204,205}

The FcRn column was coated with FcRn/ β 2-microglobulin and the antibody samples were applied on the column in a buffer (buffer A: 20 mM MeS, 150 mM NaCl) of pH 5.5.²⁰⁶ If the FcRn binding region of the antibody is intact, the antibody stays on the column till the buffer gets changed to a higher pH (20 mM tris/HCl, 150 mM NaCl, pH 8.8). If the sample is eluted immediately, no interaction with the column took place, indicating the FcRn attenuation mutation worked. We used this analysis method in **paper II** to confirm the effect of binding attenuation to the FcRn.

Imaging

Several different techniques are used in clinics to image the brain, such as MRI, CT, as well as PET and SPECT. Conventional imaging methods, such as MRI and CT, visualise non-specific changes in the morphology of tissue [51]. However, in the diagnosis of neurodegenerative diseases, the depiction of physiological and biochemical changes are important. For this purpose PET and SPECT are valuable methods.

PET and SPECT

Both PET and SPECT detect high energy-photons emerging through decay of an administered radiotracer. PET imaging is based on the annihilation of a positron with an electron, which produces two high-energy photons (long-wave gamma rays, 511 keV each) emitted at an angle of 180° to each other. These photons are detected by a detector ring inside a PET scanner.²⁰⁷ The PET scanner locates the annihilation event by estimating the line-of-response between the two detection sides on the ring.²⁰⁸ PET can give valuable specific information about the target and reveal the spatial distribution and quantity of the radiotracer.

SPECT imaging systems consist of a gamma camera, which detects the decay of gamma-emitting radionuclides by rotating a detector around the scanned object. Due to the design of the detector (collimator-type) only gamma-particles entering at a specific angle can be detected, which helps to

determine the point of origin, but reduces the sensitivity of the method.²⁰⁹ Both techniques are suitable for investigating the pharmacokinetic properties of radiolabelled substances, but in a clinical setting, PET imaging is more sensitive and shows a higher resolution than SPECT.^{65,68}

Brain retention was investigated with PET and SPECT with fluorine-18 and iodine-125, respectively. For **paper I**, iodine-125 was used to match the long biological half-life of the IgG based antibody ligand. Mice were scanned in a nanoScan SPECT/CT one hour before, one hour and one day after CA injection. For **paper III** and **IV**, PET was used to investigate the organ retention to analyse the *in vivo* behaviour of either fluorine-18 labelled antibodies or two fluorine-18 labelled tetrazines.

Brain distribution of radiolabelled antibodies

To visualise the distribution of an injected radiolabelled antibody in relation to specific brain vasculature and pathologic lesions in histological preparations, immunostaining methods as well as different autoradiography methods were used.

Immunostaining

Immunostaining describes a method to visualise proteins in *post mortem* tissue by using antibodies. First, frozen brain tissue were cryosectioned in coronal or sagittal orientation. Cryosectioning describes the process of slicing small fractions of a frozen brain tissue at -20°C. Depending on the protocol, the tissue was fixated with 4% paraformaldehyde or ice-cold methanol. Further, the unspecific binding sites need to be masked by using a blocking buffer, which done by using serum. After application and incubation with a primary antibody that binds the target of interest, a secondary antibody, usually connected to a fluorophore, was applied to detect the primary antibody, and thereby the target structure, under a microscope. This method was used in **paper I** and **II**.

Autoradiography

Autoradiography is based on the detection of radioactivity in a tissue by a phosphor imaging plate. Phosphor imaging is a robust, yet sensitive method for the quantification of tissue sections treated with radiolabelled compounds,²¹⁰ either directly applied to the tissue *in vitro* or administered *in vivo*. Imaging plates are photostimulable phosphor screens on a plastic base, or more simply spoken, a phosphor which can store images. Typically it is build out of four layers, a protective plastic layer, a photostimulable phosphor layer, a polyester support layer and a plastic backbone. The most important layer of the plate is the phosphor layer, which contains a [BaF (Br0.85, I 0.15)

: Eu^{2+}] crystal mixed with a binder.²¹¹ When ionising radiation is absorbed Eu^{2+} is losing an electron, which is trapped in the crystal.^{212,213} A He-Ne laser can excite the trapped electrons and an emission of blue light can be detected. This process is called photostimulated luminescence.²¹⁴

To perform *ex vivo* autoradiography, coronal or sagittal brain cryosections from mice injected with a radiolabelled antibody were exposed to phosphor-imaging plates. The exposure time varied depending on the type and amount of radioisotope used in the studies.

Nuclear track emulsion

Nuclear track emulsion (NTE) or microautoradiography is used to provide an image of the distribution of a radioactive compound on cellular level. It was established in the 1970s^{215,216} and relies on direct exposure of a radioactive tissue sample to a photographic emulsion.²¹⁰ The great benefit of NTE is the more detailed localisation of the radioactive compound in tissue samples and it was used in **paper I** and **II**.

A microscopic slide containing a coronal or sagittal brain section was immunostained with antibodies visualising brain targets of interest, in this case $\text{A}\beta$ and the vascular marker CD31, then submerged in nuclear emulsion. The emulsion contains silver halide crystals, like silver bromide (AgBr), which after exposure to ionising radiation form a cluster of silver atoms that are visible after development of the emulsion. The ionising radiation absorbed by the silver halide crystals releases free electrons and creates electron deficient bromine atoms. This movement of electrons, in combination with free silver ions, forms a cluster of four or more silver atoms and creates a latent image centre, which can be reduced to metallic silver during development.²¹⁷

Aims

The overall aim of this thesis was to improve antibody based imaging in the brain, by increasing the contrast and shorten the time between tracer injection and imaging. To achieve this, various strategies to enhance the peripheral clearance of an antibody-based imaging ligand, as well as exploring *in vivo* pre-targeting possibilities were investigated. The specific aims were the following:

In **paper I**, we compared two peripheral clearing approaches with each other to assess their effect on antibody-based SPECT imaging. For this we modified antibodies either via attachment of a mannose-residue for direct clearance or by using a two-step induced clearing approach, based on the IEDDA reaction.

In **paper II** we wanted to investigate the reduction of the biological half-life of two different antibodies, achieved by protein engineering to attenuate the neonatal Fc-receptor binding. Further, we wanted to characterise their *in vivo* behaviour in WT and AD mouse models (App^{NL-G-F}) and evaluate their potential for immunoPET applications.

In **paper III** we radiolabelled the leading antibody candidates of **paper II** with fluorine-18 to evaluate them with PET imaging. We thus aimed to analyse their uptake over a time course of 9 h and in addition, to try to discriminate between WT and AD mouse models (App^{NL-G-F}) 12 h after antibody injection.

In **paper IV** we aimed to develop novel radiolabelled tetrazines for pre-targeting applications. Specifically, two tetrazines with similar structure were fluorine-18 labelled and evaluated *in vivo* with PET imaging to assess their pharmacokinetic properties.

Summary of Paper I-IV

Paper I

In **Paper I**, two peripheral clearing approaches were compared to assess their effect on antibody-based SPECT-imaging.

The A β -binding antibody RmAb158 and its bispecific, brain penetrating version RmAb158-scFv8D3 were functionalised for liver-targeted clearance by two different methods. The first method involved the attachment of a mannose sugar molecule, which served to interact with the liver to result in direct clearance of the antibody from blood. The second method involved modifying the antibodies with TCO moieties and inducing clearance through the injection of a CA three days after antibody injection. The CA was based on albumin and functionalised with tetrazines, for interaction with the TCO-functionalised antibody, as well as galactose for liver targeted excretion.

The antibodies were radiolabelled with iodine-125 and injected into wildtype (WT) or AD mice (tg-ArcSwe). The mice injected with mannose-modified antibody were sacrificed after 24 h. For the induced clearing strategy the antibodies were left to circulate *in vivo* for three days before the clearance was induced by injection of a CA. Mice which were selected for induced clearance were imaged with SPECT at 72 h after antibody injection, as well as 2 h and 24 h after CA administration. The clearance of the antibodies was monitored with blood sampling throughout the experimental period and quantified by measurement of radioactivity in the blood samples.

None of the clearing strategies worked well with the bispecific RmAb158-scFv8D3 antibody, as the plasma availability of this antibody was too low, due to interaction with TfR on blood cells. The direct clearing strategy via mannose did not look promising for RmAb158, as the antibody was cleared too fast to allow sufficient brain accumulation. However, we could show that the induced clearing strategy substantially lowered the blood concentration of [¹²⁵I]I-RmAb158 already at 2 h after CA administration, allowing us to image the antibody in the brain with increased contrast at an earlier time point, thus enabling us to show a proof-of-concept.

In conclusion, an increased contrast was demonstrated by combining an antibody-based imaging tracer with an induced clearing strategy, setting the foundation for future induced clearing strategies with different antibody ligands.

Paper II

In **Paper II**, the reduction in the biological half-life of antibodies was investigated by attenuating their binding to the neonatal Fc-receptor (FcRn) for potential use in immunoPET. Two bispecific, brain penetrating antibodies and two regular, monospecific IgG versions were designed, all based on the A β -binding, humanised antibody Bapineuzumab (Bapi). The two bispecific antibodies (Bapi-Fab8D3) were designed with knob-into-hole technique to enable monovalent recombinant fusion of the TfR antibody fragment Fab8D3 to the C-terminus of one of the heavy chains. The other two antibodies (Bapi) were of regular monospecific IgG design. One bispecific and one monospecific antibody contained a two amino acid mutation (HAHQ) to lower the binding to FcRn, which plays a crucial role for the biological half-life of antibodies. The introduction of this mutation (FcRn-) thus aimed to decrease the antibodies' residence time in blood. After production, the antibodies were assessed for quality and binding to A β , TfR and FcRn. To evaluate the influence of the FcRn mutation on blood clearance and brain penetration, the four antibodies were radiolabelled with iodine-125 and injected in WT mice. Blood concentrations of the antibodies were assessed at 5 and 30 min, as well as 2, 6, 24, 48, 72 and 170 h after injection. Brain concentrations were measured *ex vivo* at 3 h or 7 days after injection. Finally, the two bispecific constructs (Bapi-Fab8D3 and Bapi-Fab8D3^{FcRn-}) were radiolabelled and injected into WT and AD mice (*App*^{NL-G-F}) to assess the influence of the FcRn mutation on the brain, blood and peripheral organ biodistribution at 12 h and 24 h after injection.

Ex vivo evaluation of the four antibodies in WT mice showed a clear difference in brain uptake between the bispecific and monospecific antibody constructs 3 h after administration. When assessed over a seven day period, blood concentrations of the antibodies with the FcRn mutation declined substantially faster than the non-mutated variants and thus clearly reduced their biological half-life. We could calculate the blood half-lives of the antibodies to the following: Bapi^{FcRn-}: 4.5 h, Bapi: 23.7 h, Bapi-Fab8D3^{FcRn-}: 4.5 h, Bapi-Fab8D3: 22.3 h. The 24 h study in WT and *App*^{NL-G-F} mice showed a significantly higher brain retention in *App*^{NL-G-F} mice compared to WT mice. Importantly, the relative retention of Bapi-Fab8D3^{FcRn-} in *App*^{NL-G-F} mice was considerably higher compared with the non-mutated Bapi-Fab8D3, which means more antibody was in the brain, in relation to the blood. This brain-to-blood ratio is an important factor to evaluate if the accumulation of a radiotracer, and therefore its signal, will be higher than the background provided by the residual tracer in the blood. Already 12 h after injection, Bapi-Fab8D3^{FcRn-} displayed a higher brain-to-blood ratio in *App*^{NL-G-F} compared with WT mice.

In conclusion the FcRn mutated antibodies showed rapid blood elimination and high brain uptake. Reducing the biological half-life by mutating the FcRn

binding of an antibody resulted in a high brain-to-blood ratio and discrimination between AD and WT mice already 12 h after antibody administration. This is a promising step to make antibody-based PET imaging feasible for clinical use. By decreasing the residence time of antibodies in the blood and increasing the brain-to-blood ratio, the FcRn mutated antibodies have the potential to provide better contrast and diagnostic accuracy for imaging A β pathology in AD patients. Further optimization and investigation of these modified antibodies may contribute to the development of more effective diagnostic tools for Alzheimer's disease and other neurodegenerative disorders.

Paper III

In **Paper III**, *in vivo* PET was performed to evaluate the pharmacokinetics of fluorine-18 labelled antibodies with attenuated neonatal Fc-receptor binding, as well as their ability to detect and quantify A β pathology in *App*^{NL-G-F} mice. The bispecific Bapi-Fab8D3^{FcRn-} and the regular monospecific Bapi^{FcRn-} from **paper II** were functionalised with TCO and radiolabelled with a fluorine-18 labelled tetrazine for PET imaging. A total of six WT mice per antibody were injected with the radiolabelled antibodies and PET scanned in an alternating manner, resulting in brain PET data for 3 mice per time point with almost complete coverage over 9 h after the first injection. Time shifted injections allowed for blood sampling at 5 and 30 min, as well as 1, 2, 3, 4, 6 and 7 h post injection of mice that were not currently in the scanner. All animals were euthanized 9 h after injection. Terminal blood, brains and peripheral organs were extracted and the biodistribution of the two antibodies were compared. Time-activity curves (TAC) of the antibodies were extracted from the PET images and compared to each other. Based on findings in **paper II**, a second PET experiment was performed, where 3 WT and 3 *App*^{NL-G-F} mice were injected with [¹⁸F]F-Bapi-Fab8D3^{FcRn-} and scanned 12 h after antibody injection. *Ex vivo* measurements of brain, blood and peripheral organs were extracted, measured and compared.

The *in vivo* dynamics of the FcRn mutated antibodies were visualised with alternating PET scans, to obtain a nearly complete coverage of the total brain concentration of [¹⁸F]F-Bapi^{FcRn-} and [¹⁸F]F-Bapi-Fab8D3^{FcRn-} over a 9 h period. PET data demonstrated that while total brain concentration of [¹⁸F]F-Bapi^{FcRn-} started to decline immediately after injection, [¹⁸F]F-Bapi-Fab8D3^{FcRn-} initially displayed a stable brain concentration, followed by drop and then a slow decline. Blood sampling showed that both antibodies were eliminated from blood at a rate that closely mirrored the PET derived brain elimination of [¹⁸F]F-Bapi^{FcRn-}, suggesting its PET signal primarily reflected concentration in blood, whereas the PET signal of [¹⁸F]F-Bapi-Fab8D3^{FcRn-} reflected also a significant brain uptake due to TfR mediated transport over the BBB. Indeed, when PET data was compared with the measurements of

post mortem brain retention, [^{18}F]Bapi-Fab8D3^{FcRn} displayed a ten-fold higher uptake compared to [^{18}F]Bapi^{FcRn}. Finally, PET imaging was conducted in *App*^{NL-G-F} and WT mice 12 h after injection of [^{18}F]Bapi-Fab8D3^{FcRn}. Higher standard uptake values (SUV) were recorded in *App*^{NL-G-F} mice, but due to the small group size, the difference did not reach significance (p values were 0.10, 0.09 and 0.07 for whole brain, cortex and hippocampus, respectively). Since the A β pathology of *App*^{NL-G-F} mice is spread throughout the whole brain, it is difficult to find a suitable internal reference region for normalisation, by the use of an SUV ratio. However, when [^{18}F]Bapi-Fab8D3^{FcRn} retention was instead normalised to terminal blood concentrations, obtained immediately after scanning, variation between animals was considerably reduced. The resulting brain-to-blood ratio was thus significantly higher in all assessed brain regions of *App*^{NL-G-F} compared to WT.

To conclude, antibody-based imaging is a promising method to image A β pathology. This study showed the *in vivo* dynamics of the TfR mediated transport of a bispecific antibody into the brain. In addition, a mutation of the antibody's FcRn binding allowed for the quantification of A β pathology and discrimination between AD from WT mice with immunoPET imaging already 12 h after antibody administration. This study brings us an additional step towards development of a clinically useful method for immunoPET imaging in the brain.

Paper IV

In **Paper IV**, two tetrazines were radiolabelled with fluorine-18 to evaluate their potential for pre-targeting. Pre-targeting describes the concept of combining the high specificity of antibodies with the fast kinetics of small molecules. A typical sequence of events would be the injection of an antibody, modified with a small molecule, such as a TCO which is allowed to circulate for few days to accumulate at the target and to be cleared from the periphery. In a second step a small, fluorine-18 labelled tetrazine with fast kinetics and homogenous brain distribution is injected and forms a covalent bond with the TCO-group of the antibody to enable visualisation of the antibody.

Two compounds, a methyl tetrazine (MeTz) and an H-tetrazine (HTz) were selected based on their lipophilicity. A small molecule aimed for brain-penetration has to have a balance of lipophilicity and hydrophilicity in order to penetrate the BBB without remaining in the brain. Both tetrazines were radiolabelled using a two-step procedure via [^{18}F]F-Py-TFP, synthesized on solid support followed by amidation with amine-bearing tetrazines. PET imaging was performed in WT and tg-ArcSwe mice to assess the brain pharmacokinetic properties of the tetrazines. To determine their suitability for *in vivo* pre-targeting, they should enter the brain in high concentrations and then be rapidly cleared from the brain tissue. Time-activity curves were derived from the

PET images and analysed to evaluate the potential of the tetrazines to be used for pre-targeting.

Both compounds, [^{18}F]MeTz and [^{18}F]HTz were successfully radiolabelled resulting in radiochemical yields of 24% and 22%, respectively, and a radiochemical purity of > 96%. The corresponding reference compounds were synthesised and the structures were confirmed via NMR.

The PET scans in mice showed that both [^{18}F]MeTz and [^{18}F]HTz were able to cross the BBB and reach the brain. Following PET scans, TACs of [^{18}F]MeTz and [^{18}F]HTz from in the whole brain, cortex, hippocampus and cerebellum were extracted. Both labelled tetrazines displayed a maximum concentration (C_{max}) in the whole brain within the first minute, followed by a gradual decline over the 60 min scanning time. [^{18}F]MeTz had a higher brain uptake compared [^{18}F]HTz, suggesting that [^{18}F]MeTz crossed the BBB more efficiently. But even though [^{18}F]MeTz entered the brain to a larger extent within the first five minutes, both were clearance from the brain to a similar concentration, making them promising candidates for further pre-targeted PET imaging evaluation.

Antibody-based therapy for Alzheimer's disease is in development, and therefore we need suitable diagnostic methods to screen for the target in the brain and to monitor the effect of therapy. The fluorine-18 labelled tetrazines evaluated in this study may become important tools for future development of pre-targeted imaging of A β in AD.

Results and discussion

Increased peripheral clearance

Several factors are influencing the biological half-life of an antibody. In this thesis the antibody size, the functionality of its Fc domain, chemical modifications, as well as the TfR affinity and valency were described.

Our research group has investigated immunoPET with TfR bearing antibodies in multiple studies over the past decade.^{25,70,71,73,108,109,125,218} Several different antibody designs have been explored¹²⁵ (Fig. 6.) and explained in regards to their potential for immunoPET. An important aspect to consider is the time between injection and imaging, as it influences the radiation dose the patient will receive, as well as the resolution, by providing a favourable signal-to-noise ratio. The smallest antibody construct designed in our lab showed the best pharmacokinetic profile for immunoPET, which allowed imaging one day after injection.⁷³ However, this antibody format suffered from low production yields and instability issues, which is why larger antibody constructs might be more beneficial. However, due to their larger size and interactions with the FcRn, which governs the recirculation of antibodies, the biological half-life of full IgG radiotracers is less favourable. As an example, in previous studies from our group we could show that an iodine-125 labelled IgG antibody (RmAb158) can be imaged in the brain up to 27-days post injection (p.i.), but a favourable target-to-background ratio was only achieved after 14-days.¹⁰⁹ As described in the paper, the slow peripheral clearance of the antibody resulted in noisy SPECT images up to 14 days p.i. Thus, as stated in one of our previous papers, “the difficulties with antibody based radiolig-

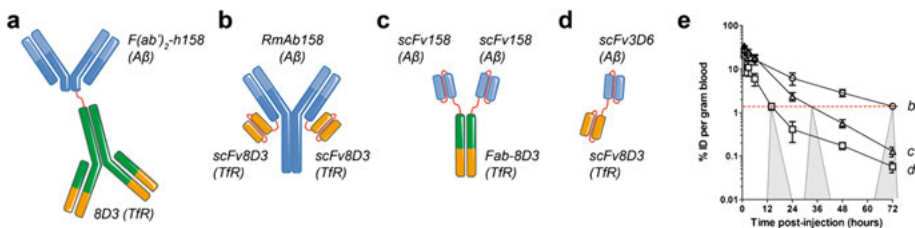


Figure 6 Antibody designs of our group **A** 8D3-F(ab')₂-h158 **B** RmAb158-scFv8D3 **C** Tribody **D** di-scFv3D6-8D3 **E** blood concentration curves (%ID/g) show decreasing half-lives in relation to antibody size. From Sehlin *et al.*, 2019

ands is [...] not the extent of brain delivery per se but rather the slow elimination from blood".¹⁰⁸ A faster blood-clearance can be achieved not only by reducing the size of the antibody, but also by using active clearing strategies from the blood.

In **Paper I**, the antibody RmAb158 was chemically modified with mannose for enhanced clearance by targeting liver receptors. To visualise the behaviour of the antibody in the blood, it was radiolabelled with iodine-125. A clear effect on mannose- ^{125}I -RmAb158 was observed, already 5 min after injection. At this time point, the concentration of mannose- ^{125}I -RmAb158 was on average 12 %ID/g compared to 27 %ID/g for the non-mannosylated ^{125}I -RmAb158. At 24 h p.i. blood concentration of mannose- ^{125}I -RmAb158 had decreased to 0.6 %ID/g, compared to 6 %ID/g for ^{125}I -RmAb158. This indicated that mannose modified RmAb158 was cleared from the blood substantially faster than unmodified RmAb158 and that the clearance was efficient already at the earliest studied time point. To reduce the blood-circulation time this method worked excellently, however the clearance was too effective, resulting in a lower brain-uptake, compared to the non-mannosylated control. This highlights the important balance between clearance and uptake.

In addition, another strategy was examined, which involved induced clearance via a CA. The idea of induced clearance is not new; however, it has primarily been explored for cancer imaging or therapy purposes.^{197,219–221} In **Paper I**, an iodine-125 radiolabelled antibody, modified with TCO, was injected into mice. Three days later, the albumin-based CA, modified with tetrazine to promote IEDDA conjugation with the TCO, was injected to promote clearance via the liver. Blood sampling throughout the experiment showed that the radioactivity signal in blood dropped immediately after injection of the CA, indicating a rapid clearance effect. Consequently, we also observed a considerably higher radioactive signal in the liver of mice euthanized 1.5 h after CA administration compared to non-injected animals, which is in line with the expected mechanism of action. Indeed, the induced clearing strategy did prove the intended principle, as it reduced the time between antibody administration and SPECT imaging for RmAb158.

However, for the imaging to work properly, higher antibody brain concentrations must be achieved. Therefore, the bispecific, brain-penetrating RmAb158-scFv8D3 was also studied in **Paper I**. RmAb158-scFv8D3 was largely unaffected by both strategies to enhance blood clearance. Consequently, an additional experiment was performed hypothesizing that the effect of both clearing strategies could be dependent on the fraction of free antibody in plasma. Thus, ^{125}I -RmAb158-scFv8D3 and ^{125}I -RmAb158 were injected in mice and the amount of radioactivity in plasma was compared with that in total blood and in blood cell pellet. The result showed that only 10–20% of ^{125}I -RmAb158-scFv8D3 was free in plasma and the rest was bound to blood cells, while ^{125}I -RmAb158 was more available in plasma, with around 90% found in the plasma fraction. Previous studies in the research group

showed that a stronger affinity to TfR resulted in a lower plasma availability,^{74,222,223} most likely due to their binding to TfR on blood cells, as seen in **paper I**, and to TfR in peripheral organs and tissues. Further, the properties of the TfR-binders will affect these interactions, such that high affinity or avidity will increase binding to TfR, leading to faster clearance from blood and subsequent degradation.

Increased peripheral clearance can be provided by modifying the antibody by adding sugar-residues, as discussed above, or by genetic modification of the antibody properties. In **Paper II**, the blood-clearance of an antibody with a modified protein sequence was explored to reduce the binding to the FcRn, which is important for the re-circulation of an antibody *in vivo*. To investigate this effect, the biological half-lives of [¹²⁵I]I-Bapi, [¹²⁵I]I-Bapi^{FcRn-}, [¹²⁵I]I-Bapi-Fab8D3 and [¹²⁵I]I-Bapi-Fab8D3^{FcRn-} in WT mice were analysed. In WT mice, the influence of the FcRn attenuation on blood clearance and brain penetration could be studied without the influence of an intrabrain target. Both antibodies with the FcRn mutation displayed an increased clearance from the blood, compared with their non-mutated variants. This influence was visible already 6 h post injection and displayed a clear separation after 24 h. The FcRn mutation reduced the biological half-life to be 5-times shorter, compared to the non-mutated control, resulting in a biological half-life of 4.5 h of [¹²⁵I]I-Bapi^{FcRn-}, compared to 23.7 h of [¹²⁵I]I-Bapi and 4.5 h for [¹²⁵I]I-Bapi-Fab8D3^{FcRn-}, compared to 22.3 h of [¹²⁵I]I-Bapi-Fab8D3. Interestingly, although the non-mutated [¹²⁵I]I-Bapi-Fab8D3 displayed faster clearance than [¹²⁵I]I-Bapi, due to its interaction with the TfR,^{89,224} the mutated variants had almost identical pharmacokinetics. At the end of the experiment, seven days after injection, both antibodies with the FcRn mutation showed an overall lower total blood concentration. The effect of the mutation was especially evident for the antibodies without TfR-binder, which displayed a large difference in blood concentration and is in line with previous studies on the influence of the FcRn on the biological half-life of antibodies.^{138,225–230} Besides mutations lowering antibodies' affinity to the FcRn, a CA binding to the FcRn-binding region on the antibody, called Abdeg, has been developed^{231,232} and is currently in a clinical trial to be evaluated for therapeutic applications.²³³

Reverse Gatekeeping – you shall not leave?

Apart from regulating the antibody blood concentrations, FcRn has been postulated to have additional functions. In 2005, a study showed that A β binding antibodies had a slower brain clearance in FcRn knockout animals.²³⁴ In several studies^{235–237} the FcRn has been hypothesised to promote efflux of IgG molecules over the BBB, from brain to blood. Therefore, the mutation of the FcRn binding on the antibody molecule could increase the accumulation of antibodies in the brain over time either via the extended retention time in the

brain, or via enhanced peripheral clearance. Both paths could improve the target-to-background ratio and thereby the contrast in immunoPET. It has been shown that the FcRn is expressed at the BBB,²³⁵ but the theory of FcRn promoted efflux is controversial.^{238–240} In **paper II** we concluded that the FcRn mutation substantially increased blood clearance of Bapi^{FcRn-} and Bapi-Fab8D3^{FcRn-}. We could also see that these antibodies showed an overall higher brain-to-blood ratio compared to the non-mutated controls, seven days after administration. This study was conducted in WT mice, which raised the question whether this could be caused by interaction with an intrabrain target. Neurons express TfR,²⁴¹ which could explain the longer brain retention and higher brain-to-blood ratio of the TfR-binding antibodies. However, it does not explain why both Bapi^{FcRn-} and Bapi-Fab-8D3^{FcRn-} had significantly higher brain-to-blood ratio compared to their non-mutated variants. Looking at the data in more detail, it can be concluded that the faster blood clearance is most certainly responsible for the higher target-to-background ratio of the FcRn binding mutated antibodies.

Further studies in **paper II** investigated the brain distribution 12 h and 24 h after injection in WT, compared to AD disease model mice (*App*^{NL-G-F}). Due to the target engagement of antibody in *App*^{NL-G-F} mice with A β , a higher brain-to-blood ratio compared with WT mice could be observed. At 24 h after injection, the brain retention of [¹²⁵I]-Bapi-Fab8D3 was about twice as high as that of [¹²⁵I]-Bapi-Fab8D3^{FcRn-} in *App*^{NL-G-F} mice. However, the difference between *App*^{NL-G-F} and WT mice was only 3-fold for [¹²⁵I]-Bapi-Fab8D3, while the mutated [¹²⁵I]-Bapi-Fab8D3^{FcRn-} displayed 14-fold higher brain concentration in *App*^{NL-G-F} compared with WT mice. [¹²⁵I]-Bapi-Fab8D3 clearly showed a higher accumulation in *App*^{NL-G-F} and WT mice than [¹²⁵I]-Bapi-Fab8D3^{FcRn-}, which is likely caused by a higher total plasma concentration and therefore more influx into the brain. However, the brain-to-blood ratio was around 5-fold higher for [¹²⁵I]-Bapi-Fab8D3^{FcRn-} than for [¹²⁵I]-Bapi-Fab8D3 in *App*^{NL-G-F} mice, which could be a better indicator for achieving PET images with a high signal-to-noise.

One click to success?

Since the development of the inverse electron-demand Diels–Alder (IEDDA) cycloaddition in 2008 a fast click reaction was born, giving the possibility to explore the functions of TCO and tetrazine in living systems further.¹⁸⁰ Clearing agents have been explored previously and can be used to disable the TCO reactivity in the blood, then referred to as masking agents.²⁴² According to this principle only target-accumulated TCO will be selected by a radiolabelled tetrazine, as the TCO of the peripheral circulating TCO-bearing agent is not available or gets cleared from the blood by additional functional groups on the clearing agent.^{197,243–246} In **paper I** we studied a clearing agent which is based on albumin and functionalised with tetrazines, for interaction with the TCO-

functionalised antibody in the blood, as well as galactose for liver targeted excretion. Blood sampling over time could demonstrate an immediate effect of the CA, showing its fast reaction kinetics *in vivo*. The very same CA we used in **paper I** was successfully demonstrated to increase the tumour-to-blood ratio.¹⁹⁷ We could show that the administration of the same CA for an intrabrain target can increase the contrast in SPECT-imaging, proving its use not only for tumour-imaging, but also for applications within the CNS. Several other studies have investigated clearing agents, based on dextran polymers. These increase the imaging contrast, but show nonspecific binding in other organs, making them not yet functional for clinical applications.^{221,246} The CA used in **paper I** shows great potential, but it should be kept in mind that the disadvantage of promoted liver clearance of a radioactive compound should be further assessed, as the extended retention could cause liver damage.

The IEDDA is a promising approach to combine the specificity of antibodies and the fast reaction-kinetics of a small molecule, commonly called pre-targeting. Pre-targeting in the periphery was shown in the past¹⁸³ and has also been explored beyond the BBB.^{184,247–249} A common issue with TCO-modifications is the isomerisation of TCO to CCO in blood by transition metals.²⁵⁰ **Paper I** taught us that the TCO that was attached to the antibody was functional *in vivo* up to three days post injection. This is important when this antibody-TCO combination is considered for future pre-targeting approaches, where the TCO-functionalised antibody will be allowed to circulate in the body for a number of days before injection of a fluorine-18 labelled tetrazine for detection.

Tetrazines used for pre-targeting in peripheral targets, such as tumours, need to fulfil different requirements than tetrazines which will be used for intrabrain targets. The brain is considered to be a “fatty” organ,²⁵¹ which is why a compound targeting the brain needs to be fairly lipophilic to pass the BBB, but not too lipophilic so that it gets stuck in the brain. In **paper IV** we tested two novel tetrazines, whose lipophilicity was calculated beforehand and was hypothesised to be of moderate lipophilicity to enter the brain but not get stuck in it.^{252,253} We could see that both tetrazines entered the brain in a fast manner and were efficiently washed out during the one hour PET-scan. Due to the higher lipophilicity, provided by one additional methyl-group, the [¹⁸F]MeTz entered the brain more efficiently, compared to the structurally equivalent [¹⁸F]HTz. However, the higher reactivity of H-tetrazines, as reported by previous studies,²⁵⁴ could be required to facilitate the coupling at the very low concentrations present *in vivo*. Therefore, a combination of the antibodies from **paper II** / **paper III** and the tetrazines presented in **paper IV** would need to be assessed in future *in vivo* experiments on pre-targeting in the CNS.

Considerations for the design of brain immunoPET ligands

Several factors influence the potential of a brain penetrating, bispecific immunoPET ligand, such as dose, pH-sensitivity, affinity and avidity or valency. Valency describes the number of binding sites between an antibody and its antigen. Here studies have shown that monovalent TfR binders pass the BBB more efficiently.^{70,193} Results from **paper I** and other studies from our group suggest that high TfR avidity may reduce plasma availability.^{74,255} Bispecific antibodies with high TfR avidity, caused by bivalent binding to TfR, may also reside longer time in the endothelial cells of the brain vasculature, and reduce transport into the brain.^{222,256} In addition, due to the avidity effect, the bivalent antibody design causes receptor clustering at the endothelial cell surface, which increases the degradation of bivalent TfR antibodies.^{96,257} Radio-labelled antibodies stuck in the endothelial cells could also give a false impression of how much of the injected dose reached the brain. Therefore, the antibody design was changed using the knob-into-hole technique for **paper II** to achieve a monovalent TfR binding antibody design (Fig. 4). Further, when the plasma concentration of the antibody is too low, the chance for RMT in the brain decreases, which is why a slightly higher injection dose can be beneficial as it will saturate the binding to blood cells and therefore increase the plasma availability. However, too high doses will saturate the TfR on the BBB endothelium and thereby decrease BBB transcytosis.¹²⁵ Another factor which is important to consider for the design of a suitable TfR-binder is its pH dependency. The bispecific antibody gets internalised after binding to TfR and dissociates from the receptor when the pH in the endosome decreases.^{258,259} Studies suggest that an antibody with a strong TfR affinity at pH 7 and a weaker affinity at pH 6 cross the BBB more efficiently.¹⁰⁶

Several radioisotopes can be used for PET-imaging and give the possibility to build a flexible toolbox, which can be chosen from, depending on the research question and availability of material. Zirconium-89 is of interest, because of its broad availability and long half-life. Moreover, it is clinically applied and possesses good physical characteristics for PET.^{260,261} A study with a zirconium-89 labelled antibody against A β (JRF/ A β N/25) showed high affinity to the target, but the antibody displayed a low brain penetration and high non-specific binding, which makes its use as imaging agent difficult.²⁶² The *ex vivo* binding pattern was similar to patterns observed by us, with the antibodies 3D6 and mAb158,^{89,263} which seem to bind to A β deposits in the brain vasculature or ventricles. In these examples, the antibody was not connected to a carrier that allows BBB passage. A recent study that used zirconium-89 with a bispecific antibody showed that the choice of chelator for brain imaging purposes is essential. Here, Aducanumab-scFab8D3 was zirconium-89 labelled by using either N-suc-DFO, DFO-NCS or DFO*. The results showed that DFO* led to a significantly higher brain retention in a pattern similar to the A β plaque distribution.¹⁷¹ It has to be taken into account that zirconium-

89 is residualizing and could therefore bias the biodistribution data, as it is unsure if the detected signal displays the position of the zirconium-89 labelled antibody or its radioactive metabolite which is retained inside cells. Such retention could thus reflect degradation of internalized antibody after binding to either A β or TfR, where the latter could occur in both WT and A β expressing mice. Nevertheless, it is interesting to see that immunoPET in the brain is possible with zirconium-89.

In **paper I to III** we have modified the antibodies via NHS-ester modification which is commonly used in research, but could be disadvantageous for clinical translation, as this type of modification targets the lysine-residue. As these are ubiquitously available on many proteins, the modification site will be unspecific and result in a heterogeneous product population, an overall unpredictable outcome and therefore differences in the respective batches. This can be prevented by the use of site-specific modification methods. Selective N-terminal modification has been thoroughly explored.²⁶⁴ Here, direct or indirect labelling paths can be selected. An example for the direct modification is the use of a His-tag to facilitate radiolabelling with technetium-99m.²⁶⁵ For the indirect approach a two-step procedure is deployed where in the first step, the N-terminus is functionalised with a click-chemistry motif or, for example a sortase A motif. For sortase A mediated site-specific modification, the antibody sequence is modified with a specific recognition motif (amino acids LPXTG) which the enzyme needs to initiate its catalytic process. In a second step, the enzyme takes another compound, equipped with oligoglycines, and attaches it to the antibody.²⁶⁶ The oligoglycine bearing compound could be anything, from a small molecule to another protein, the possibilities are unlimited. All of these methods have been explored and contain their own set of disadvantages. For example, the modification with technetium-99m using the His-tag as chelator could cause stability issues and including a sortase motif into a protein could have a negative effect on its properties.

Conclusion and future perspective

The results presented in this thesis show that enhancing the peripheral clearance is a feasible approach to get closer to realise immunoPET. **Paper I** demonstrated that certain clearing approaches (mannosylation) worked too effectively and is therefore unsuitable for neuroPET applications. The induced clearing strategy from the same paper showed promise for a monospecific antibody that was not designed to enter the brain via RTM. However, combining the antibodies from **paper II** and the induced clearing strategy would be an interesting future experiment to remove the peripheral antibody even further. The results of this paper show that 12 h to 24 h could be a suitable time point to do PET imaging with the FcRn attenuated variant. But it would be interesting to see how a slightly increased dose, leading to higher plasma availability, in combination with a clearing agent would influence the brain delivery of the monovalent antibody with and without FcRn binding mutation. Maybe the time between injection and imaging could be shortened below 12 h, which means a study investigating different time points for CA injection might be of interest.

Further, in **paper II** we could conclude that the attenuation to the FcRn has the potential to provide better contrast for brain targeted antibodies. It would be interesting to initiate a therapy study and use the antibodies from **paper II** and **III** for longitudinal monitoring of the therapy effect and compare it to an established small molecule tracer, such as PiB. It would also be interesting to investigate if the antibody-tracer can detect the effect of the therapeutic antibody, or if the therapy antibody would block the binding-site of the tracer.

Combining the antibodies from **paper II** and **III** with a PET-isotope of longer half-life, such as iodine-124, could give additional insights into the optimal imaging time point of these antibodies. The idea of FcRn mediated efflux is intriguing and could be further explored by mutating a bispecific antibody with no target in the brain and compare the uptake and elimination with the antibodies used in **paper II** and **III** or combining the antibodies with a residualizing radioisotope, such as zirconium-89. If an antibody is radio-labelled with an iodine radioisotope, the current position of the antibody can be determined, but due to its non-residualizing properties, not the path the antibody took. We have used iodine-125 and fluorine-18, which are both non-residualizing, meaning that after being internalized and degraded, they will be

secreted from cells and washed out of the brain. The use of residualizing radioisotopes for RMT could give valuable insights for example about lysosomal degradation of the antibody in various cell types.

Another future experiment should explore the combination of the antibodies of **paper II/III** and the tetrazines of **paper IV** to test them for their potential in pre-targeting. First, it would be important to explore how many TCOs are necessary to produce a feasible PET image. Here, it would be interesting to modify the antibodies either via TCO-NHS-ester or a site-specific approach, such as using sortase A, and compare them. The advantage of the latter is that we would know the exact number and location of TCOs on the antibody, which would improve reproducibility of the method. Next, the amount of antibody in the brain required to achieve a PET signal would need to be assessed. Interestingly, Bapi-Fab8D3 from **paper II**, seemed to display increased brain concentration at 24 h after injection. This is different from antibodies previously explored in our group, and could suggest that an even longer circulation time, e.g. three days, would further increase brain retention of Bapi-Fab8D3. It is possible that the introduction of the effector function mutation LALA-PG has a positive effect on the brain retention of this antibody as it would not be cleared as fast as non-mutated antibodies from the brain. Therefore, it might show an advantageous *in vivo* behaviour for pre-targeting approaches, compared to their control.

Finally, combining the antibodies with the tetrazines from **paper IV** would allow to explore their pre-targeting potential *in vivo*. It is reported in literature that the lipophilicity and reactivity of tetrazines are inversely correlated.²⁵⁴ Therefore, it would be important to investigate whether the potentially higher reactivity of the [¹⁸F]HTz would match the higher brain uptake of the [¹⁸F]MeTz, when used as a pre-targeting agent. Depending on the results, a combination with the induced clearance from **paper I** may also be an interesting strategy to investigate.

Popular Science Summary

The brain is the control centre of the body, which is why diseases of the brain affect the entire body. In order to be able to treat a disease of the brain, it is necessary to diagnose the disease at an early stage and to follow the success of the treatment. For brain tumours, some methods have already been developed that make it possible to visualise them. But diseases like Alzheimer's are caused by misfolded proteins (called A β) that accumulate in the brain. This requires other diagnostic methods. There are already some ways to detect Alzheimer's, but they are not ideal. One way is to inject a small radioactive molecule called [^{11}C]PiB which binds at the centre of the protein deposits, called plaques, and makes it possible to image them using positron emission tomography (PET). However, these plaques are not necessarily responsible for the symptoms of Alzheimer's, and this small molecule therefore does not represent the whole dynamics in the development of the disease.

What is needed are imaging techniques that reliably show the neurotoxic accumulation products of A β . This is not so easy because the brain is a much protected area due to the blood-brain barrier. However, suitable antibodies have a great potential for use in diagnostics because they are very specific for their target. Especially if they are designed to enter the brain. To make this possible, a strategy has been developed called the "molecular Trojan horse". This involves using a small molecule attached to the antibodies to enable them to cross the blood-brain barrier.

Antibodies generally have a long residence time in the body, which is good for their innate task of fighting pathogens, but an obstacle for imaging. Especially since antibodies are labelled with radioisotopes for diagnostic purposes and the half-life of these must match the antibody's residence time in the body, which, thereby, increases the radiation exposure to the body. However there are several approaches to solving this problem. For example, one can try to shorten the residence time of the radiolabelled antibody in the body by attaching a small molecule called *trans*-cyclooctene (TCO) to the antibody, which can thereby react or bind only to a small molecule called tetrazine. This property can be used to one's advantage by additionally linking the tetrazine to a clearing agent. This CA has the ability to filter the antibody out of the blood and thus highlight it in the brain. This method is described in **paper I**.

It is also possible to shorten the residence time of the antibody by mutating the site in the antibody that is needed to extend the residence time. See **paper**

II and **paper III**. It was seen that the residence time in the blood was five times shorter compared to non-mutated controls, but the antibody was still able to enter the brain.

Another strategy to take advantage of the long retention time in the body is to use a specific strategy called pre-targeting. These are chemical reactions that occur very quickly and do not interact with anything else in the body. One of these pre-targeting methods is called the inverse-demand diels-alder reaction. In this reaction, two functional groups are involved, a tetrazine with a TCO. The TCO should be coupled to the antibody, because without the protective properties of the antibody it may lose its reactive properties in the organism. This antibody can now circulate in the body for several days and attach to its target structure without any negative effects. However, in order to visualise the position of the antibody and thus visualise the pathology, we need the second component of the reaction, a tetrazine. This tetrazine can now be labelled with a radioisotope that has a shorter half-life, because in the ideal case the tetrazine enters the brain quickly, binds to the TCO and the excess tetrazine leaves the body quickly. Once the tetrazine has bound to the TCO, the position of the antibody in the body can be visualised using PET imaging.

But some research is needed here. The tetrazine needs to have certain properties so that it can enter the brain quickly without getting stuck in the brain. This has mainly to do with the high fat content of the brain, which is why different tetrazines were tested in **paper IV** and evaluated for their potential in the laboratory.

Populärwissenschaftliche Zusammenfassung

Das Gehirn ist die Schaltzentrale des Körpers, weshalb Erkrankungen des Gehirns den kompletten Körper beeinflussen. Um eine Erkrankung des Gehirns behandeln zu können ist es erforderlich die Erkrankung frühzeitig zu diagnostizieren und den Behandlungserfolg zu verfolgen. Für Gehirntumore sind bereits einige Methoden entwickelt worden, die es ermöglichen diese darzustellen. Doch Krankheiten, wie Alzheimer entstehen durch fehlgefaltete Proteine (mit dem Namen A β), welche sich im Gehirn anreichern. Dafür sind andere diagnostische Methoden erforderlich. Es gibt bereits einige Wege die es ermöglichen Alzheimer festzustellen, doch sind sie nicht ideal. Eine Möglichkeit besteht darin, ein kleines radioaktives Molekül, [^{11}C]PiB genannt, im Zentrum der Proteinablagerungen, sogenannten Plaques, einzubringen und diese mittels Positron Emission Tomographie (PET) darzustellen. Doch sind diese Plaques nicht unbedingt für die Symptome von Alzheimer verantwortlich, und dieses kleine Molekül bildet daher nicht die ganze Dynamik in der Entwicklung der Krankheit ab.

Benötigt werden bildgebende Verfahren, welche die neurotoxischen Akkumulationsprodukte von A β zuverlässig darstellen. Das ist gar nicht so einfach, weil das Gehirn durch die Bluthirnschranke ein sehr geschützter Bereich ist. Doch haben geeignete Antikörper ein grosses Potential für den Einsatz in der Diagnostik, da sie sehr spezifisch fuer Ihr Ziel sind. Vor allem, wenn sie designed wurden um in das Gehirn zu gelangen. Um dies zu ermöglichen wurde eine Strategie entwickelt, welches das „molekulare Trojanische Pferd“ genannt wird. Hierfür benutzt man ein kleines Molekül welches an den Antikörpern befestigt wird um ihnen zu ermöglichen, die Bluthirnschranke zu überqueren.

Unglücklicherweise haben Antikörper im Allgemeinen eine lange Verweilzeit im Körper, welches gut ist fuer ihre angeborene Aufgabe, die Bekämpfung von Krankheitserregern, doch ein Hindernis für die Bildgebung. Vor allem, da Antikörper fuer die Diagnostik mit Radioisotopen markiert werden und die Halbwertszeit dieser mit der Verweilzeit des Antikörpers im Körper uebereinstimmen muss, was allerdings die Strahlenbelastung auf den Körper erhöht. Doch es gibt mehrere Lösungsansätze fuer dieses Problem. Man kann z.B. versuchen die Verweildauer des radiomarkierten Antikörpers im Körper zu verkuerzen indem man ein kleines Molekül mit dem Namen *trans*-cyclooctene (TCO) an den Antikörper befestigt. Dieses TCO wird sich nur mit

einem Tetrazin verknuepfen. Diese Eigenschaft kann man zum eigenen Vorteil verwenden, indem das Tetrazin zusätzlich mit einem Clearingagent (CA) verbunden wird. Dieser CA hat die Fähigkeit den Antikörper aus dem Blut zu filtern und somit im Gehirn hervorzuheben. Diese Methode ist in **paper I** beschrieben.

Man kann die Verweilzeit des Antikörpers auch dadurch verkürzen, indem man die Stelle im Antikörper mutiert, welche für die Verlängerung der Verweilzeit benötigt wird. Siehe dazu **paper II** und **paper III**. Man konnte sehen, dass die Verweildauer im Blut funef mal kleiner war, im Vergleich zu nicht mutierten Kontrollen, aber der Antikörper dennoch ins Gehirn gelangen konnte.

Eine weitere Strategie, um sich die lange Verweildauer im Körper zu Nutzen zu machen ist das Anwenden einer bestimmten Strategie, welche sich pre-targeting (etwa: Zielfindung- und -markierung) nennt. Hierbei handelt es sich um chemische Reaktionen, welche sehr schnell ablaufen und im Körper mit nichts anderem interagieren. Eine dieser pre-targeting Methoden wird Inverse-demand Diels-Alder (IEDDA) Reaktion genannt. In dieser Reaktion sind zwei funktionelle Gruppen beteiligt, ein Tetrazin mit einem TCO. Das TCO sollte an den Antikörper gekoppelt werden, da es ohne die schützenden Eigenschaften des Antikörpers seine reaktiven Eigenschaften im Organismus verlieren kann. Dieser Antikörper kann nun für mehrere Tage im Körper zirkulieren und sich an seiner Zielstruktur anlagern, ohne dass dies negative Effekte hat. Doch um die Position des Antikörpers darzustellen und damit die Pathologie darzustellen benötigen wir die zweite Komponente der Reaktion, ein Tetrazin. Dieses Tetrazin kann nun mit einem Radioisotop markiert werden, welches eine kürzere Halbwertszeit hat, da im idealsten Fall das Tetrazine schnell ins Gehirn eindringt, sich an das TCO bindet und das überschuessige Tetrazin den Körper schnell wieder verlässt. Sobald sich das Tetrazin an das TCO gebunden hat, kann die Position des Antikörpers im Körper mit Hilfe von PET-Bildgebung dargestellt werden.

Doch hier wird einiges an Forschung benötigt. Das Tetrazin muss bestimmte Eigenschaften vorweisen können, damit es schnell in das Gehirn kann, ohne dass es im Gehirn stecken bleibt. Das hat vor allem mit dem hohen Fett-Gehalt des Gehirns zu tun, weshalb in **paper IV** verschiedene Tetrazine geprüft und im Labor auf ihr Potential evaluiert wurden.

Funding

The work in this thesis was performed at the Department of Public Health and Caring Sciences, in the Molecular Geriatrics group, Rudbeck Laboratory, Uppsala University, Sweden. The molecular imaging work in this thesis was performed at the SciLifeLab Pilot Facility for Preclinical PET-MRI, a Swedish nationally available imaging platform at Uppsala University, Sweden, financed by the Knut and Alice Wallenberg Foundation. I would like to thank the funding bodies for financial support and travel grants over the years, including the Swedish Research Council, the Swedish Innovation Agency, Alzheimersfonden, Hjärnfonden, Torsten Söderbergs stiftelse, Åhlénstiftelsen, Hedlunds stiftelse, Konung Gustaf V:s och Drottning Victorias frimuares-tiftelse, Magnus Bergvalls stiftelse, Stiftelsen för gamla tjänarinnor and Stohnes stiftelse. This project has received funding from the European Union's Horizon 2020 research and innovation programme under the Marie Skłodowska-Curie grant agreement no 813528.

Schematic illustrations were created by the author using Biorender.com

Acknowledgments

It's incredible how fast four years can go by. With ups and downs I am very happy I finished this extremely exciting chapter of my life.

First and foremost I would love to thank my main supervisor **Dag Sehlin**. Without your support and colourful discussion my PhD would not have been possible. I appreciated your availability and that we could talk about science or bread at any given moment. I hope my baking and ELISA skills will levy to your magnitude at some point in time.

Thank you very much **Jonas Eriksson** for taking some of the radiation dose for me, because you were just much faster with your long arms. I really enjoyed talking to you in the PET centre about many different topics. Thank you for improving my radiochemistry knowledge.

Johanna Rokka – even though you left me for new opportunities in Finland, I appreciate very much all the skills you taught me in the radiolab! I hope the future looks bright and colourful for you!

Thank you **Stina** for hosting nice gatherings at your beautiful house and teaching me how to inject mice properly. You are a great inspiration for every ambitious woman.

Many thanks to **Raffaella Rossin** and **Marc Robillard** from Tagwors Pharmaceuticals for providing me with the clearing agent!

Many thanks to **Matthias Herth** and **Umberto Battisti** for all the nice consortium times and providing me with one of the tetrazines.

Thank you **Luke Odell** for investing your time to explain the NMR to me and for supervising me when I played being a chemist in your lab.

Thank you, **Martin**, for explaining interesting medical facts to me and also for letting me show of my muscle strengths.

Thank you **Abdul**, **Amelia** and **Elin** for making the last few months in the lab a very enjoyable experience. **Chiara**, I am very happy I could share an office with you for such a long time and get to know you on a personal level. I really enjoyed every minute of it! Thank you to **Anish** for always knowing all the important information, no matter if science or politics you know what is going on. Thank you **Emma** for just being awesome. It was really great to work in the same lab as you, **Evangelos**. Your eloquence and confidence is without equal. Thank you **Gillian** for some nice trips together and sharing your insanely organised google maps flags with me. The time in Uppsala would have surely been greyer without you. **Jinar**, thank you for being a great inspiration for everybody and always a pleasure to talk to. **Rebecca**, I would love to continue our music sessions ☺ Thank you **Sahar** for being a great role model! Thank you **Tiffany** for being the cute soul that you are. I am happy I could take care of you a bit in the lab and teach you some bits and pieces. Thank you **Sara** for just being interesting, interested and letting me ask very stupid questions. **Tobias**, I am really, really sad that I cannot be with you in the same office anymore. You are the man of 1000 noises and it was a very fun time to hang out all the time! Thank you **Wojciech** for being a great inspiration and also letting me walk with your dog ☺

Thank you **Ximena** for being the soul of the lab. Without you, many things would be so much more chaotic. Thank you **Mengfei**, **Elnaz**, **Khalid**, **Anna** and **Vilmantas** for being great conversations partners in the lab.

Many thanks to **Ken** – another intimidating and extremely inspiring person. You taught me so much at my short time at BioArctic. I hope one day I will be just as skilled as you are ☺

Thanks to the Dresden crew. **Moore**, my start in Sweden would have been so much more stressful if you'd have not distracted me from the distance with many movie nights and skype session. Thank you for teaching me proper English, so I could do my PhD somewhere outside of Germany. **Guillermi**, my friend! You are the most insane and inspiring person I know. I will never reach your skiing or cooking level, but that is fine by me. Everybody needs a guy like you, especially in times of distress to remind oneself of their strengths and to get some strong kicks in their butt! Thank you for being awesome! **Thomas**, the master of backhanded compliments. Without you I'd have never known about the PhD position in Sweden. I was very happy you were in the same consortium as me and we could share some good moments. **Ivan** you little cutie! Thank you for your random calls and just for being you! Your cute little baby can only become amazing!

Thank you so much **Katrín** for giving our friendship baby a chance. I am happy you waited for me! You are one of the best things that has happened to

me in Sweden. Many thanks to **José** and **George** for trying to upgrade my Bachata level.

Danke auch an **Natasa** für die vielen schönen Tage in Stockholm und Uppsala. Es freut mich, dass die Franzosen dich nicht halten konnten ☺

What would I have done the last few months without you, **Miriam**? You literally kept me sane. Thank you for all the nice conversations and just for being the awesome person you are! To **Mahdi** and **Hadi** I would like to address the warmest appreciation for creating some magical memories in Sweden.

Auch meiner Familie Danke ich von ganzem Herzen. Meine Brüder **Alex** und **Bernd** für die vielen intelligenten Gespräche als wir jünger waren, ohne die ich mit Sicherheit niemals angefangen hätte zu studieren. Jeder von euch beiden hat viele kleine Dinge zu meiner persönlichen Entwicklung beigetragen und ihr wisst es selber bestimmt nicht mal.

Leonie, für mich gehörst du schon seit einer langen Zeit zur Familie. Ich bin froh, dass wir uns nie aus den Augen verloren haben und so viele lebendige Momente miteinander teilen konnten.

Die herzlichsten aller Dankeschöne gehen an meinen **Vater** – vielen Dank für die täglichen Telefonate über Gott und die Welt. Es freut mich, dass du endlich auf meine medizinischen Ratschläge hörst ☺ Es war mir eine Freude dir Schweden näher zu bringen.

An meine herzallerliebste **Schwester** richte ich die liebsten Worte. Du bist eine Bereicherung meines Lebens und das selbige wäre so viel deprimierender würde es dich nicht geben. Was bin ich froh meine beste Freundin in der Familie zu haben. Du hast die aller süssesten Kinder auf der ganzen Welt und dein Ehemann ist auch ganz fabelhaft.

Vielen Dank auch an meine liebe **Mama**, die immer sehr gerne und viel über ihre Kinder erzählt hat – ob man es hören wollte oder nicht. Du erzählst bestimmt immernoch über uns, leider nur an einem Ort an dem wir dich nicht erreichen können.

And last, but not least, I would love to thank **Merlin** – my family cat! You are the most amazing creature and always purr when it's needed. Nothing is as cuddly as you and I love you with all my heart.

References

1. Association, A. & others. 2020 Alzheimer's disease facts and figures. *Alzheimer's Dement.* **16**, 391–460 (2020).
2. Sachdev, P. S. *The Ageing Brain. The Neurobiology and Neuropsychiatry of Ageing.* (Swets & Zeitlinger B.V, 2003).
3. Dai, M. H., Zheng, H., Zeng, L. D. & Zhang, Y. The genes associated with early-onset Alzheimer's disease. *Oncotarget* **9**, 15132 (2018).
4. Jack, C. R. *et al.* Tracking pathophysiological processes in Alzheimer's disease: an updated hypothetical model of dynamic biomarkers. *Lancet. Neurol.* **12**, 207–216 (2013).
5. Palmqvist, S. *et al.* Cerebrospinal fluid and plasma biomarker trajectories with increasing amyloid deposition in Alzheimer's disease. *EMBO Mol. Med.* **11**, (2019).
6. De Silva, H. A. R. *et al.* Cell-specific expression of beta-amyloid precursor protein isoform mRNAs and proteins in neurons and astrocytes. *Brain Res. Mol. Brain Res.* **47**, 147–156 (1997).
7. Hur, J. Y. γ -Secretase in Alzheimer's disease. *Exp. Mol. Med.* **2022** *544* **54**, 433–446 (2022).
8. JARRETT, J. T., BERGER, E. P. & LANSBURY, P. T. The C-terminus of the beta protein is critical in amyloidogenesis. *Ann. N. Y. Acad. Sci.* **695**, 144–148 (1993).
9. Marina, G. B. *et al.* Amyloid β -protein (A β) assembly: A β 40 and A β 42 oligomerize through distinct pathways. *Proc. Natl. Acad. Sci. U. S. A.* **100**, 330 (2003).
10. Hardy, J. A. & Higgins, G. A. Alzheimer's disease: the amyloid cascade hypothesis. *Science* **256**, 184–185 (1992).
11. Glenner, G. G. & Wong, C. W. Alzheimer's disease: initial report of the purification and characterization of a novel cerebrovascular amyloid protein. *Biochem. Biophys. Res. Commun.* **120**, 885–890 (1984).
12. Selkoe, D. J. & Hardy, J. The amyloid hypothesis of Alzheimer's disease at 25 years. *EMBO Mol. Med.* **8**, 595–608 (2016).
13. Morley, J. E. *et al.* A physiological role for amyloid-beta protein: enhancement of learning and memory. *J. Alzheimers. Dis.* **19**, 441–449 (2010).
14. Puzzo, D. *et al.* Endogenous amyloid- β is necessary for hippocampal synaptic plasticity and memory. *Ann. Neurol.* **69**, 819–830 (2011).

15. Puzzo, D. *et al.* Picomolar amyloid-beta positively modulates synaptic plasticity and memory in hippocampus. *J. Neurosci.* **28**, 14537–14545 (2008).
16. Flood, J. F., Morley, J. E. & Roberts, E. Amnestic effects in mice of four synthetic peptides homologous to amyloid beta protein from patients with Alzheimer disease. *Proc. Natl. Acad. Sci. U. S. A.* **88**, 3363 (1991).
17. Flood, J. F., Morley, J. E. & Roberts, E. An amyloid beta-protein fragment, A beta[12-28], equipotently impairs post-training memory processing when injected into different limbic system structures. *Brain Res.* **663**, 271–276 (1994).
18. Morley, J. E. & Farr, S. A. The role of amyloid-beta in the regulation of memory. *Biochem. Pharmacol.* **88**, 479–485 (2014).
19. Morley, J. E. & Farr, S. A. Hormesis and amyloid- β protein: physiology or pathology? *J. Alzheimers. Dis.* **29**, 487–492 (2012).
20. Atwood, C. S., Bowen, R. L., Smith, M. A. & Perry, G. Cerebrovascular requirement for sealant, anti-coagulant and remodeling molecules that allow for the maintenance of vascular integrity and blood supply. *Brain Res. Rev.* **43**, 164–178 (2003).
21. Morley, J. E., Farr, S. A., Nguyen, A. D. & Xu, F. What is the Physiological Function of Amyloid-Beta Protein? *J. Nutr. Heal. Aging* **23**, 225–226 (2019).
22. Bishop, G. M. & Robinson, S. R. Physiological roles of amyloid-beta and implications for its removal in Alzheimer's disease. *Drugs Aging* **21**, 621–630 (2004).
23. Soscia, S. J. *et al.* The Alzheimer's disease-associated amyloid beta-protein is an antimicrobial peptide. *PLoS One* **5**, (2010).
24. Asher, S. & Priefer, R. Alzheimer's disease failed clinical trials. *Life Sci.* **306**, (2022).
25. Meier, S. R. *et al.* 11 C-PiB and 124 I-Antibody PET Provide Differing Estimates of Brain Amyloid- β After Therapeutic Intervention. *J. Nucl. Med.* **63**, 302–309 (2022).
26. Can BACE Inhibitors Stage a Comeback? | ALZFORUM. Available at: <https://www.alzforum.org/news/conference-coverage/can-bace-inhibitors-stage-comeback>. (Accessed: 21st March 2023)
27. Cai, Z. *et al.* Role of RAGE in Alzheimer's Disease. *Cell. Mol. Neurobiol.* **2015 364 36**, 483–495 (2015).
28. Evaluation of the Efficacy and Safety of Azeliragon (TTP488) in Patients With Mild Alzheimer's Disease - Full Text View - ClinicalTrials.gov. Available at: <https://clinicaltrials.gov/ct2/show/NCT02080364>. (Accessed: 21st March 2023)
29. Panza, F., Lozupone, M., Seripa, D. & Imbimbo, B. P. Amyloid- β immunotherapy for alzheimer disease: Is it now a long shot? *Ann. Neurol.* **85**, 303–315 (2019).

30. FDA. FDA Grants Accelerated Approval for Alzheimer's Disease Treatment. *January 06, 2023* (2023). Available at: <https://www.fda.gov/news-events/press-announcements/fda-grants-accelerated-approval-alzheimers-disease-treatment>.
31. Cavazzoni, P. (FDA C. for D. E. and R. FDA's Decision to Approve New Treatment for Alzheimer's Disease. *FDA's Decision to Approve New Treatment for Alzheimer's Disease* (2021). Available at: <https://www.fda.gov/drugs/news-events-human-drugs/fdas-decision-approve-new-treatment-alzheimers-disease>.
32. Sperling, R. A. *et al.* Amyloid-related imaging abnormalities in amyloid-modifying therapeutic trials: Recommendations from the Alzheimer's Association Research Roundtable Workgroup. *Alzheimer's Dement.* **7**, 367–385 (2011).
33. Bapineuzumab Phase 3: Target Engagement, But No Benefit | ALZFORUM. Available at: <https://www.alzforum.org/news/conference-coverage/bapineuzumab-phase-3-target-engagement-no-benefit>. (Accessed: 22nd March 2023)
34. Plotkin, S. S. & Cashman, N. R. Passive immunotherapies targeting A β and tau in Alzheimer's disease. *Neurobiol. Dis.* **144**, 105010 (2020).
35. Rofo, F. *et al.* Novel multivalent design of a monoclonal antibody improves binding strength to soluble aggregates of amyloid beta. *Transl. Neurodegener.* *2021 101* **10**, 1–16 (2021).
36. van Dyck, C. H. *et al.* Lecanemab in Early Alzheimer's Disease. *N. Engl. J. Med.* **388**, (2023).
37. Sevigny, J. *et al.* The antibody aducanumab reduces A β plaques in Alzheimer's disease. *Nature* **537**, 50–56 (2016).
38. Beshir, S. A. *et al.* Aducanumab Therapy to Treat Alzheimer's Disease: A Narrative Review. *Int. J. Alzheimers. Dis.* **2022**, (2022).
39. Vaz, M., Silva, V., Monteiro, C. & Silvestre, S. Role of Aducanumab in the Treatment of Alzheimer's Disease: Challenges and Opportunities. *Clin. Interv. Aging* **17**, 797–810 (2022).
40. Mahase, E. Three FDA advisory panel members resign over approval of Alzheimer's drug. *BMJ* **373**, n1503 (2021).
41. Knopman, D. S., Jones, D. T. & Greicius, M. D. Failure to demonstrate efficacy of aducanumab: An analysis of the EMERGE and ENGAGE trials as reported by Biogen, December 2019. **17**, 696–701 (2021).
42. Loureiro, J. C. *et al.* Passive anti-amyloid immunotherapy for Alzheimer's disease. *Curr. Opin. Psychiatry* **33**, 284–291 (2020).
43. Gleason, A., Ayton, S. & Bush, A. I. Unblinded by the light: amyloid-related imaging abnormalities in Alzheimer's clinical trials. *Eur. J. Neurol.* **28**, e1–e1 (2021).
44. Whittington, M. D. *et al.* Cost-Effectiveness and Value-Based Pricing of Aducanumab for Patients With Early Alzheimer Disease. *Neurology* **98**, E968–E977 (2022).

45. Abbott, N. J. Evidence for bulk flow of brain interstitial fluid: Significance for physiology and pathology. *Neurochem. Int.* **45**, 545–552 (2004).
46. Iliff, J. J. *et al.* A paravascular pathway facilitates CSF flow through the brain parenchyma and the clearance of interstitial solutes, including amyloid β . *Sci. Transl. Med.* **4**, (2012).
47. Olsson, B. *et al.* CSF and blood biomarkers for the diagnosis of Alzheimer's disease: a systematic review and meta-analysis. *Lancet. Neurol.* **15**, 673–684 (2016).
48. Hansson, O., Lehmann, S., Otto, M., Zetterberg, H. & Lewczuk, P. Advantages and disadvantages of the use of the CSF Amyloid β (A β) 42/40 ratio in the diagnosis of Alzheimer's Disease. *Alzheimers. Res. Ther.* **11**, 1–15 (2019).
49. Hampel, H., Goernitz, A. & Buerger, K. Advances in the development of biomarkers for Alzheimer's disease: From CSF total tau and A β 1-42 proteins to phosphorylated tau protein. *Brain Res. Bull.* **61**, 243–253 (2003).
50. Neselius, S. *et al.* CSF-biomarkers in Olympic boxing: diagnosis and effects of repetitive head trauma. *PLoS One* **7**, (2012).
51. Tapiola, T. *et al.* Cerebrospinal fluid {beta}-amyloid 42 and tau proteins as biomarkers of Alzheimer-type pathologic changes in the brain. *Arch. Neurol.* **66**, 382–389 (2009).
52. Shea, D. *et al.* SOBA: Development and testing of a soluble oligomer binding assay for detection of amyloidogenic toxic oligomers. *Proc. Natl. Acad. Sci. U. S. A.* **119**, (2022).
53. Mielke, M. M. *et al.* Plasma phospho-tau181 increases with Alzheimer's disease clinical severity and is associated with tau- and amyloid-positron emission tomography. *Alzheimer's Dement.* **14**, 989–997 (2018).
54. Thijssen, E. H. *et al.* Diagnostic value of plasma phosphorylated tau181 in Alzheimer's disease and frontotemporal lobar degeneration. *Nat. Med.* **2020 263 26**, 387–397 (2020).
55. Janelidze, S. *et al.* Plasma P-tau181 in Alzheimer's disease: relationship to other biomarkers, differential diagnosis, neuropathology and longitudinal progression to Alzheimer's dementia. *Nat. Med.* **2020 263 26**, 379–386 (2020).
56. Lantero Rodriguez, J. *et al.* Plasma p-tau181 accurately predicts Alzheimer's disease pathology at least 8 years prior to post-mortem and improves the clinical characterisation of cognitive decline. *Acta Neuropathol.* **140**, 267–278 (2020).
57. Karikari, T. K. *et al.* Blood phosphorylated tau 181 as a biomarker for Alzheimer's disease: a diagnostic performance and prediction modelling study using data from four prospective cohorts. *Lancet Neurol.* **19**, 422–433 (2020).
58. Benussi, A. *et al.* Diagnostic and prognostic value of serum NfL and

- p-Tau181 in frontotemporal lobar degeneration. *J. Neurol. Neurosurg. Psychiatry* **91**, 960–967 (2020).
59. Palmqvist, S. *et al.* Discriminative Accuracy of Plasma Phospho-tau217 for Alzheimer Disease vs Other Neurodegenerative Disorders. *JAMA* **324**, 772–781 (2020).
 60. Gonzalez-Ortiz, F. *et al.* Brain-derived tau: a novel blood-based biomarker for Alzheimer’s disease-type neurodegeneration. *Brain* **146**, 1152–1165 (2023).
 61. Klunk, W. E. *et al.* Imaging Brain Amyloid in Alzheimer’s Disease with Pittsburgh Compound-B. *Ann. Neurol.* **55**, 306–319 (2004).
 62. Wu, C., Bowers, M. T. & Shea, J.-E. On the origin of the stronger binding of PIB over thioflavin T to protofibrils of the Alzheimer amyloid- β peptide: a molecular dynamics study. *Biophys. J.* **100**, 1316–1324 (2011).
 63. Anand, K. & Sabbagh, M. Amyloid Imaging: Poised for Integration into Medical Practice. *Neurotherapeutics* **14**, 54 (2017).
 64. Lansbury, P. T. & Lashuel, H. A. A century-old debate on protein aggregation and neurodegeneration enters the clinic. *Nature* **443**, 774–779 (2006).
 65. Hicks, R. J. & Hofman, M. S. Is there still a role for SPECT-CT in oncology in the PET-CT era? *Nat. Rev. Clin. Oncol.* **9**, 712 (2012).
 66. Engler, H. *et al.* Two-year follow-up of amyloid deposition in patients with Alzheimer’s disease. *Brain* **129**, 2856–2866 (2006).
 67. Glabe, C. G. & Kaye, R. Common structure and toxic function of amyloid oligomers implies a common mechanism of pathogenesis. *Neurology* **66**, S74–S78 (2006).
 68. Rahmim, A. & Zaidi, H. PET versus SPECT: strengths, limitations and challenges. *Nucl. Med. Commun.* **29**, 193–207 (2008).
 69. Philpott, G. W. *et al.* RadioimmunoPET: Detection of Colorectal Carcinoma with Positron-Emitting Copper-64-Labeled Monoclonal Antibody. *J. Nucl. Med.* **36**, 1818–1824 (1995).
 70. Hultqvist, G., Syvänen, S., Fang, X. T., Lannfelt, L. & Sehlin, D. Bivalent brain shuttle increases antibody uptake by monovalent binding to the transferrin receptor. *Theranostics* **7**, 308–318 (2017).
 71. Sehlin, D. *et al.* Antibody-based PET imaging of amyloid beta in mouse models of Alzheimer’s disease. *Nat. Commun.* **7**, 1–11 (2016).
 72. Syvänen, S. *et al.* Fluorine-18-Labeled Antibody Ligands for PET Imaging of Amyloid- β in Brain. *ACS Chem. Neurosci.* **11**, 4460–4468 (2020).
 73. Fang, X. T. *et al.* High detection sensitivity with antibody-based PET radioligand for amyloid beta in brain. *Neuroimage* **184**, 881–888 (2019).
 74. Bonvicini, G. *et al.* ImmunoPET imaging of amyloid-beta in a rat model of Alzheimer’s disease with a bispecific, brain-penetrating fusion protein. *Transl. Neurodegener.* **11**, (2022).

75. Meier, S. R. *et al.* Antibody-Based In Vivo PET Imaging Detects Amyloid- β Reduction in Alzheimer Transgenic Mice After BACE-1 Inhibition. **59**, (2018).
76. Meier, S. R. *et al.* 11C-PiB and 124I-Antibody PET Provide Differing Estimates of Brain Amyloid- β After Therapeutic Intervention. *J. Nucl. Med.* **63**, 302–309 (2022).
77. Meier, S. R., Sehlin, D., Hultqvist, G. & Syvänen, S. Pinpointing Brain TREM2 Levels in Two Mouse Models of Alzheimer’s Disease. *Mol. imaging Biol.* **23**, 665–675 (2021).
78. Meier, S. R., Sehlin, D. & Syvänen, S. Passive and receptor mediated brain delivery of an anti-GFAP nanobody. *Nucl. Med. Biol.* **114–115**, 128–134 (2022).
79. Roshanbin, S. *et al.* In vivo imaging of alpha-synuclein with antibody-based PET. *Neuropharmacology* **208**, (2022).
80. Chowdhury, E. A. *et al.* Understanding the brain uptake and permeability of small molecules through the BBB: A technical overview. *J. Cereb. Blood Flow Metab.* 0271678X20985946 (2021). doi:10.1177/0271678X20985946
81. Liu, X., Tu, M., Kelly, R. S., Chen, C. & Smith, B. J. Development of a computational approach to predict blood-brain barrier permeability. *Drug Metab. Dispos.* **32**, 132–139 (2004).
82. Schdev, P. S. *The Neurobiology and Neuropsychiatry of Ageing.* (Swets and Zeitlinger B.V., Lisse, The Netherlands, 2003).
83. Liebner, S., Czapalla, C. J. & Wolburg, H. Current concepts of blood-brain barrier development. *Int. J. Dev. Biol.* **55**, 467–476 (2011).
84. Furuse, M., Fujita, K., Hiiragi, T., Fujimoto, K. & Tsukita, S. Claudin-1 and-2: novel integral membrane proteins localizing at tight junctions with no sequence similarity to occludin. *J. Cell Biol.* **141**, 1539–1550 (1998).
85. Chen, G. F. *et al.* Amyloid beta: structure, biology and structure-based therapeutic development. *Acta Pharmacol. Sin.* **38**, 1205–1235 (2017).
86. Bard, F. *et al.* Peripherally administered antibodies against amyloid beta-peptide enter the central nervous system and reduce pathology in a mouse model of Alzheimer disease. *Nat. Med.* **6**, 916–919 (2000).
87. Roshanbin, S. *et al.* Reduction of α SYN Pathology in a Mouse Model of PD Using a Brain-Penetrating Bispecific Antibody. *Pharmaceutics* **14**, (2022).
88. Sehlin, D. *et al.* Brain delivery of biologics using a cross-species reactive transferrin receptor 1 VNAR shuttle. *FASEB J.* **34**, 13272–13283 (2020).
89. Syvänen, S. *et al.* Efficient clearance of A β protofibrils in A β PP-transgenic mice treated with a brain-penetrating bifunctional antibody. *Alzheimers. Res. Ther.* **10**, (2018).
90. Boado, R. J. *et al.* Pharmacokinetics and brain uptake of a genetically engineered bifunctional fusion antibody targeting the mouse

- transferrin receptor. *Mol. Pharm.* **7**, 237–244 (2010).
91. Kariolis, M. S. *et al.* Brain delivery of therapeutic proteins using an Fc fragment blood-brain barrier transport vehicle in mice and monkeys. *Sci. Transl. Med.* **12**, (2020).
 92. Ullman, J. C. *et al.* Brain delivery and activity of a lysosomal enzyme using a blood-brain barrier transport vehicle in mice. *Sci. Transl. Med.* **12**, (2020).
 93. Johnson, Kaspar Bendix; Burkhart Annette; Thomsen, Louiza Bohn; Andresen, Thomas Lars; Moos, T. Targeting the transferrin receptor for brain drug delivery.
 94. Montemiglio, L. C. *et al.* Cryo-EM structure of the human ferritin–transferrin receptor 1 complex. *Nat. Commun.* **2019 101** **10**, 1–8 (2019).
 95. Chiou, B., Neely, E. B., Mcdevitt, D. S., Simpson, I. A. & Connor, J. R. Transferrin and H-ferritin involvement in brain iron acquisition during postnatal development: impact of sex and genotype. *J. Neurochem.* **152**, 381–396 (2020).
 96. Niewoehner, J. *et al.* Increased Brain Penetration and Potency of a Therapeutic Antibody Using a Monovalent Molecular Shuttle. *Neuron* **81**, 49–60 (2014).
 97. Yu, Y. J. *et al.* Therapeutic bispecific antibodies cross the blood-brain barrier in nonhuman primates. *Sci. Transl. Med.* **6**, (2014).
 98. Yu, Y. J. *et al.* Boosting brain uptake of a therapeutic antibody by reducing its affinity for a transcytosis target. *Sci. Transl. Med.* **3**, (2011).
 99. Edavettal, S. *et al.* Enhanced delivery of antibodies across the blood-brain barrier via TEMs with inherent receptor-mediated phagocytosis. *Med* **3**, 860-882.e15 (2022).
 100. Villaseñor, R., Schilling, M., Sundaresan, J., Lutz, Y. & Collin, L. Sorting Tubules Regulate Blood-Brain Barrier Transcytosis. *Cell Rep.* **21**, 3256–3270 (2017).
 101. Zhao, P. *et al.* Enhanced anti-angiogenetic effect of transferrin receptor-mediated delivery of VEGF-trap in a glioblastoma mouse model. *MAbs* **14**, (2022).
 102. Arguello, A. *et al.* Molecular architecture determines brain delivery of a transferrin receptor–targeted lysosomal enzyme. *J. Exp. Med.* **219**, (2022).
 103. Haqqani, A. S. *et al.* Endosomal trafficking regulates receptor-mediated transcytosis of antibodies across the blood brain barrier. doi:10.1177/0271678X17740031
 104. Bien-Ly, N. *et al.* Transferrin receptor (TfR) trafficking determines brain uptake of TfR antibody affinity variants. *J. Exp. Med.* **211**, 233–244 (2014).
 105. Couch, J. A. *et al.* Addressing safety liabilities of TfR bispecific antibodies that cross the blood-brain barrier. *Sci. Transl. Med.* **5**,

- (2013).
106. Sade, H. *et al.* A Human Blood-Brain Barrier Transcytosis Assay Reveals Antibody Transcytosis Influenced by pH-Dependent Receptor Binding. *PLoS One* **9**, e96340 (2014).
 107. Kissel, K. *et al.* Immunohistochemical localization of the murine transferrin receptor (TfR) on blood--tissue barriers using a novel anti-TfR monoclonal antibody. *Histochem. Cell Biol.* **110**, 63–72 (1998).
 108. Syvänen, S. *et al.* A bispecific Tribody PET radioligand for visualization of amyloid-beta protofibrils--a new concept for neuroimaging. *Neuroimage* **148**, 55–63 (2017).
 109. Gustavsson, T., Syvänen, S., O’Callaghan, P. & Sehlin, D. SPECT imaging of distribution and retention of a brain-penetrating bispecific amyloid- $\beta\beta$ antibody in a mouse model of Alzheimer’s disease. *Transl. Neurodegener.* **9**, 1–11 (2020).
 110. Imai, K., Yachi, A. & Ferrone, S. Preparation and characterization of monoclonal antibodies to human melanoma-associated antigens (MAA). in *The Radioimmunochemical Detection of Cancer* 141–150 (Masson Publishing USA, New York, 1982).
 111. Ryman, J. T. & Meibohm, B. Pharmacokinetics of monoclonal antibodies. *CPT pharmacometrics Syst. Pharmacol.* **6**, 576–588 (2017).
 112. Wei, W. *et al.* ImmunoPET: Concept, Design, and Applications. (2020). doi:10.1021/acs.chemrev.9b00738
 113. Ward, E. S., Zhou, J., Ghetie, V. & Ober, R. J. Evidence to support the cellular mechanism involved in serum IgG homeostasis in humans. *Int. Immunol.* **15**, 187–195 (2003).
 114. Ober, R. J., Martinez, C., Vaccaro, C., Zhou, J. & Ward, E. S. Visualizing the site and dynamics of IgG salvage by the MHC class I-related receptor, FcRn. *J. Immunol.* **172**, 2021–2029 (2004).
 115. Suzuki, T. *et al.* Importance of neonatal FcR in regulating the serum half-life of therapeutic proteins containing the Fc domain of human IgG1: a comparative study of the affinity of monoclonal antibodies and Fc-fusion proteins to human neonatal FcR. *J. Immunol.* **184**, 1968–1976 (2010).
 116. Könnig, D. *et al.* Camelid and shark single domain antibodies: structural features and therapeutic potential. *Curr. Opin. Struct. Biol.* **45**, 10–16 (2017).
 117. Yan, J., Li, G., Hu, Y., Ou, W. & Wan, Y. Construction of a synthetic phage-displayed Nanobody library with CDR3 regions randomized by trinucleotide cassettes for diagnostic applications. *J. Transl. Med.* **12**, 1–12 (2014).
 118. Muyldermans, S. Nanobodies: natural single-domain antibodies. *Annu. Rev. Biochem.* **82**, 775–797 (2013).
 119. Chakravarty, R., Goel, S. & Cai, W. Nanobody: The “Magic Bullet” for Molecular Imaging? *Theranostics* **4**, 386–398 (2014).

120. Pruszynski, M. *et al.* Improved tumor targeting of anti-HER2 nanobody through N-succinimidyl 4-guanidinomethyl-3-iodobenzoate radiolabeling. *J. Nucl. Med.* **55**, 650–656 (2014).
121. Behr, T. M., Goldenberg, D. M. & Becker, W. Reducing the renal uptake of radiolabeled antibody fragments and peptides for diagnosis and therapy: present status, future prospects and limitations. *Eur. J. Nucl. Med.* **25**, 201–212 (1998).
122. Vegt, E. *et al.* Renal toxicity of radiolabeled peptides and antibody fragments: mechanisms, impact on radionuclide therapy, and strategies for prevention. *J. Nucl. Med.* **51**, 1049–1058 (2010).
123. de Vos, J., Devoogdt, N., Lahoutte, T., Muyldermans, S. & Muyldermans, S. Camelid single-domain antibody-fragment engineering for (pre)clinical in vivo molecular imaging applications: adjusting the bullet to its target. *Expert Opin. Biol. Ther.* **13**, 1149–1160 (2013).
124. Definition of bispecific antibody - NCI Dictionary of Cancer Terms - NCI. Available at: <https://www.cancer.gov/publications/dictionaries/cancer-terms/def/bispecific-antibody>. (Accessed: 13th March 2023)
125. Sehlin, D. & Syvänen, S. Engineered antibodies: new possibilities for brain PET? *Eur. J. Nucl. Med. Mol. Imaging* **11**, (2019).
126. Pommié, C., Levadoux, S., Sabatier, R., Lefranc, G. & Lefranc, M.-P. P. IMGT standardized criteria for statistical analysis of immunoglobulin V-REGION amino acid properties. **17**, 17–32 (2004).
127. IMGT Home page. Available at: <https://www.imgt.org/>. (Accessed: 28th March 2023)
128. Carter, P. Bispecific human IgG by design. *J. Immunol. Methods* **248**, 7–15 (2001).
129. Grunert, I. *et al.* Detailed Analytical Characterization of a Bispecific IgG1 CrossMab Antibody of the Knob-into-Hole Format Applying Various Stress Conditions Revealed Pronounced Stability. **7**, 3671–3679 (2022).
130. Ridgway, J. B. B., Presta, L. G. & Carter, P. ‘Knobs-into-holes’ engineering of antibody CH3 domains for heavy chain heterodimerization. *Protein Eng. Des. Sel.* **9**, 617–621 (1996).
131. Lo, M. *et al.* Effector-attenuating Substitutions That Maintain Antibody Stability and Reduce Toxicity in Mice. *J. Biol. Chem.* **292**, 3900–3908 (2017).
132. Gelderman, K. A., Tomlinson, S., Ross, G. D. & Gorter, A. Complement function in mAb-mediated cancer immunotherapy. *Trends Immunol.* **25**, 158–164 (2004).
133. Hashimoto, G., Wright, P. F. & Karzon, D. T. Antibody-Dependent Cell-Mediated Cytotoxicity Against Influenza Virus-Infected Cells. *J. Infect. Dis.* **148**, 785–794 (1983).
134. Hessell, A. J. *et al.* Fc receptor but not complement binding is

- important in antibody protection against HIV. *Nature* **449**, 101–104 (2007).
135. Sonderrmann, P., Huber, R., Oosthulzen, V. & Jacob, U. The 3.2-A crystal structure of the human IgG1 Fc fragment-Fc gammaRIII complex. *Nature* **406**, 267–273 (2000).
 136. Idusogie, E. E. *et al.* Mapping of the C1q binding site on rituxan, a chimeric antibody with a human IgG1 Fc. *J. Immunol.* **164**, 4178–4184 (2000).
 137. Simister, N. E. & Mostov, K. E. An Fc receptor structurally related to MHC class I antigens. *Nat.* 1989 3376203 **337**, 184–187 (1989).
 138. Roopenian, D. C. & Akilesh, S. FcRn: the neonatal Fc receptor comes of age. *Nat. Rev. Immunol.* **7**, 715–725 (2007).
 139. Shields, R. L. *et al.* High Resolution Mapping of the Binding Site on Human IgG1 for FcγRI, FcγRII, FcγRIII, and FcRn and Design of IgG1 Variants with Improved Binding to the FcγR. *J. Biol. Chem.* **276**, 6591–6604 (2001).
 140. Nazarova, L. *et al.* Effect of Modulating FcRn Binding on Direct and Pretargeted Tumor Uptake of Full-length Antibodies. *Mol. Cancer Ther.* **19**, 1052–1058 (2020).
 141. Yip, V. *et al.* Quantitative cumulative biodistribution of antibodies in mice: Effect of modulating binding affinity to the neonatal Fc receptor. *MAbs* **6**, 689 (2014).
 142. West, A. P. & Bjorkman, P. J. Crystal structure and immunoglobulin G binding properties of the human major histocompatibility complex-related Fc receptor(.). *Biochemistry* **39**, 9698–9708 (2000).
 143. Martin, W. L., West, A. P., Gan, L. & Bjorkman, P. J. Crystal Structure at 2.8 Å of an FcRn/Heterodimeric Fc Complex: Mechanism of pH-Dependent Binding. *Mol. Cell* **7**, 867–877 (2001).
 144. Saha, G. B. & Saha, G. B. *Fundamentals of Nuclear Pharmacy*. **6**, (Springer, 2010).
 145. Saha, G. B. *Basics of PET imaging: physics, chemistry, and regulations*. (Springer).
 146. Koehler, L., Gagnon, K., McQuarrie, S. & Wuest, F. Iodine-124: A Promising Positron Emitter for Organic PET Chemistry. *Molecules* **15**, 2686 (2010).
 147. Nye, J. A., Avila-Rodriguez, M. A. & Nickles, R. J. A new binary compound for the production of 124I via the 124Te(p,n)124I reaction. *Appl. Radiat. Isot.* **65**, 407–412 (2007).
 148. Wilson, C. B. *et al.* Quantitative measurement of monoclonal antibody distribution and blood flow using positron emission tomography and 124iodine in patients with breast cancer. *Int. J. cancer* **47**, 344–347 (1991).
 149. Divgi, C. R. *et al.* Preoperative characterisation of clear-cell renal carcinoma using iodine-124-labelled antibody chimeric G250 (124I-cG250) and PET in patients with renal masses: a phase I trial. *Lancet*.

- Oncol.* **8**, 304–310 (2007).
150. Carrasquillo, J. A. *et al.* 124I-huA33 Antibody PET of Colorectal Cancer. *J. Nucl. Med.* **52**, 1173 (2011).
 151. Divgi, C. R. *et al.* Positron Emission Tomography/Computed Tomography Identification of Clear Cell Renal Cell Carcinoma: Results From the REDECT Trial. *J. Clin. Oncol.* **31**, 187 (2013).
 152. Kuker, R., Szejnberg, M. & Gulec, S. I-124 Imaging and Dosimetry. *Mol. Imaging Radionucl. Ther.* **26**, 66 (2017).
 153. Cascini, G. L. *et al.* 124Iodine: A Longer-Life Positron Emitter Isotope—New Opportunities in Molecular Imaging. *Biomed Res. Int.* **2014**, (2014).
 154. He, P., Haswell, S. J., Pamme, N. & Archibald, S. J. Advances in processes for PET radiotracer synthesis: Separation of [18F]fluoride from enriched [18O]water. *Appl. Radiat. Isot.* **91**, 64–70 (2014).
 155. Carter, L. M. *et al.* The Impact of Positron Range on PET Resolution, Evaluated with Phantoms and PHITS Monte Carlo Simulations for Conventional and Non-conventional Radionuclides. *Mol. imaging Biol.* **22**, 73 (2020).
 156. Shukla, A. K. & Kumar, U. Positron emission tomography: An overview. **31**, 13 (2006).
 157. Vaidyanathan, G. *et al.* Preclinical Evaluation of 18F-Labeled Anti-HER2 Nanobody Conjugates for Imaging HER2 Receptor Expression by Immuno-PET. *J. Nucl. Med.* **57**, 967–973 (2016).
 158. Speranza, A. *et al.* Fully automated synthesis procedure of 4-[18F]fluorobenzaldehyde by commercial synthesizer: Amino-oxi peptide labelling prosthetic group. *Appl. Radiat. Isot.* **67**, 1664–1669 (2009).
 159. Phipps, M. D., Sanders, V. A. & Deri, M. A. Current State of Targeted Radiometal-Based Constructs for the Detection and Treatment of Disease in the Brain. *Bioconjug. Chem.* **32**, 1331–1347 (2021).
 160. Cheal, S. M. *et al.* Pairwise Comparison of 89Zr- and 124I-labeled cG250 Based on Positron Emission Tomography Imaging and Non-Linear Immunokinetic Modeling: In Vivo Carbonic Anhydrase IX Receptor Binding and Internalization in Mouse Xenografts of Clear Cell Renal Carcinoma. *Eur. J. Nucl. Med. Mol. Imaging* **41**, 985 (2014).
 161. Yang, X. *et al.* cRGD-functionalized, DOX-conjugated, and ⁶⁴Cu-labeled superparamagnetic iron oxide nanoparticles for targeted anticancer drug delivery and PET/MR imaging. *Biomaterials* **32**, 4151–4160 (2011).
 162. Lewis, J. S., Windhorst, A. D. & Zeglis, B. M. *Radiopharmaceutical Chemistry*. (Springer, 2019).
 163. Blower, J. E. *et al.* The Radiopharmaceutical Chemistry of the Radionuclides of Gallium and Indium. *Radiopharm. Chem.* 255–271 (2019). doi:10.1007/978-3-319-98947-1_14

164. W. Severin, G., W. Engle, J., E. Barnhart, T. & Nickles, R. J. ⁸⁹Zr Radiochemistry for PET. *Med. Chem.* **7**, 389 (2011).
165. La, M. T., Tran, V. H. & Kim, H. K. Progress of Coordination and Utilization of Zirconium-89 for Positron Emission Tomography (PET) Studies. *Nucl. Med. Mol. Imaging (2010)*. **53**, 115 (2019).
166. Zhang, Y., Hong, H. & Cai, W. PET Tracers Based on Zirconium-89. *Curr. Radiopharm.* **4**, 131 (2011).
167. Dilworth, J. R. & Pascu, S. I. The chemistry of PET imaging with zirconium-89. *Chem. Soc. Rev.* **47**, 2554–2571 (2018).
168. Verel, I. *et al.* ⁸⁹Zr Immuno-PET: Comprehensive Procedures for the Production of ⁸⁹Zr-Labeled Monoclonal Antibodies. *J Nucl Med* **44**, 1271–1281 (2003).
169. Vosjan, M. J. W. D. *et al.* Conjugation and radiolabeling of monoclonal antibodies with zirconium-89 for PET imaging using the bifunctional chelate p-isothiocyanatobenzyl-desferrioxamine. *Nat. Protoc.* **5**, 739–743 (2010).
170. Patra, M. *et al.* An octadentate bifunctional chelating agent for the development of stable zirconium-89 based molecular imaging probes. *Chem. Commun.* **50**, 11523–11525 (2014).
171. Wuensche, T. E. *et al.* Advancing ⁸⁹Zr-immuno-PET in neuroscience with a bispecific anti-amyloid-beta monoclonal antibody - The choice of chelator is essential. *Theranostics* **12**, 7067–7079 (2022).
172. Stéen, E. J. L. *et al.* Pretargeting in nuclear imaging and radionuclide therapy: Improving efficacy of theranostics and nanomedicines. *Biomaterials* **179**, 209–245 (2018).
173. Börjesson, P. K. E. *et al.* Radiation Dosimetry of ⁸⁹Zr-Labeled Chimeric Monoclonal Antibody U36 as Used for Immuno-PET in Head and Neck Cancer Patients. *J Nucl Med* **50**, 1828–1836 (2009).
174. Goodwin, D. A., Mears, C. F., McTigue, M. & David, G. S. Monoclonal antibody hapten radiopharmaceutical delivery. *Nucl. Med. Commun.* **7**, 569–580 (1986).
175. Goodwin, D. *et al.* Use of specific antibody for rapid clearance of circulating blood background from radiolabeled tumor imaging proteins. *Eur. J. Nucl. Med.* **9**, 209–215 (1984).
176. Knight, J. C. & Cornelissen, B. Bioorthogonal chemistry: implications for pretargeted nuclear (PET/SPECT) imaging and therapy. *Am. J. Nucl. Med. Mol. Imaging* **4**, 96–113 (2014).
177. Hang, H. C., Yu, C., Kato, D. L. & Bertozzi, C. R. A metabolic labeling approach toward proteomic analysis of mucin-type O-linked glycosylation. *Proc. Natl. Acad. Sci. U. S. A.* **100**, 14846–14851 (2003).
178. The Nobel Prize in Chemistry 2022. Available at: <https://www.nobelprize.org/prizes/chemistry/2022/summary/>. (Accessed: 13th March 2023)
179. Sletten, E. M. & Bertozzi, C. R. Bioorthogonal chemistry: Fishing for

- selectivity in a sea of functionality. *Angew. Chemie - Int. Ed.* **48**, 6974–6998 (2009).
180. Blackman, M. L., Royzen, M. & Fox, J. M. Tetrazine ligation: Fast bioconjugation based on inverse-electron-demand Diels-Alder reactivity. *J. Am. Chem. Soc.* **130**, 13518–13519 (2008).
 181. Pagel, M. Inverse electron demand Diels--Alder (IEDDA) reactions in peptide chemistry. *J. Pept. Sci.* **25**, e3141 (2019).
 182. Devaraj, N. K., Upadhyay, R., Haun, J. B., Hilderbrand, S. A. & Weissleder, R. Fast and sensitive pretargeted labeling of cancer cells through a tetrazine/trans-cyclooctene cycloaddition. *Angew. Chemie - Int. Ed.* **48**, 7013–7016 (2009).
 183. Rossin, R. *et al.* In vivo chemistry for pretargeted tumor imaging in live mice. *Angew. Chemie - Int. Ed.* **49**, 3375–3378 (2010).
 184. Shalgunov, V. *et al.* Pretargeted imaging beyond the blood-brain barrier. *RSC Med. Chem.* (2023). doi:10.1039/d2md00360k
 185. Mullan, M. *et al.* A pathogenic mutation for probable Alzheimer's disease in the APP gene at the N--terminus of β --amyloid. *Nat. Genet.* **1**, 345–347 (1992).
 186. Nilsberth, C. *et al.* The 'Arctic' APP mutation (E693G) causes Alzheimer's disease by enhanced A β protofibril formation. *Nat. Neurosci.* **4**, 887–893 (2001).
 187. Lord, A. *et al.* The Arctic Alzheimer mutation facilitates early intraneuronal A β aggregation and senile plaque formation in transgenic mice. *Neurobiol. Aging* **27**, 67–77 (2006).
 188. Philipson, O. *et al.* A highly insoluble state of A β similar to that of Alzheimer's disease brain is found in Arctic APP transgenic mice. *Neurobiol. Aging* **30**, 1393–1405 (2009).
 189. Saito, T. *et al.* Single App knock-in mouse models of Alzheimer's disease. *Nat. Neurosci.* **17**, 661–663 (2014).
 190. Sacher, C. *et al.* Longitudinal PET Monitoring of Amyloidosis and Microglial Activation in a Second-Generation Amyloid- β Mouse Model. *J. Nucl. Med.* **60**, 1787–1793 (2019).
 191. Englund, H. *et al.* Sensitive ELISA detection of amyloid- β protofibrils in biological samples. *J. Neurochem.* **103**, 334–345 (2007).
 192. Fang, X. T., Sehlin, D., Lannfelt, L., Syvänen, S. & Hultqvist, G. Efficient and inexpensive transient expression of multispecific multivalent antibodies in Expi293 cells. *Biol. Proced. Online* **19**, 1–9 (2017).
 193. Niewoehner, J. *et al.* Increased brain penetration and potency of a therapeutic antibody using a monovalent molecular shuttle. *Neuron* **81**, 49–60 (2014).
 194. Robin, B. *et al.* Blood-Brain Barrier Shuttles Containing Antibodies Recognizing Alpha-Synuclein. (2017).
 195. Sinitsyn, V. V., Mamontova, A. G., Checkneva, Y. Y., Shnyra, A. A. & Domogatsky, S. P. Rapid blood clearance of biotinylated IgG after

- infusion of avidin. *J. Nucl. Med.* **30**, 66–69 (1989).
196. Rossin, R. & Robillard, M. S. Pretargeted imaging using bioorthogonal chemistry in mice. *Curr. Opin. Chem. Biol.* **21**, 161–169 (2014).
 197. Rossin, R., Läppchen, T., Van Den Bosch, S. M., Laforest, R. & Robillard, M. S. Diels-alder reaction for tumor pretargeting: In vivo chemistry can boost tumor radiation dose compared with directly labeled antibody. *J. Nucl. Med.* **54**, 1989–1995 (2013).
 198. Rothenhäusler, B. & Knoll, W. Surface-plasmon microscopy. *Nat. 1988 3326165* **332**, 615–617 (1988).
 199. Zhu, X. & Gao, T. Spectrometry. *Nano-inspired Biosens. Protein Assay with Clin. Appl.* 237–264 (2018). doi:10.1016/B978-0-12-815053-5.00010-6
 200. Schlothauer, T. *et al.* Analytical FcRn affinity chromatography for functional characterization of monoclonal antibodies. *MAbs* **5**, 576–586 (2013).
 201. Sánchez, L. M., Penny, D. M. & Bjorkman, P. J. Stoichiometry of the interaction between the major histocompatibility complex-related Fc receptor and its Fc ligand. *Biochemistry* **38**, 9471–9476 (1999).
 202. Raghavan, M., Wang, Y. & Bjorkman, P. J. Effects of receptor dimerization on the interaction between the class I major histocompatibility complex-related Fc receptor and IgG. *Proc. Natl. Acad. Sci. U. S. A.* **92**, 11200 (1995).
 203. Martin, W. L. & Bjorkman, P. J. Characterization of the 2:1 complex between the class I MHC-related Fc receptor and its Fc ligand in solution. *Biochemistry* **38**, 12639–12647 (1999).
 204. Goebel, N. A. *et al.* Neonatal Fc receptor mediates internalization of Fc in transfected human endothelial cells. *Mol. Biol. Cell* **19**, 5490–5505 (2008).
 205. Ober, R. J., Martinez, C., Lai, X., Zhou, J. & Ward, E. S. Exocytosis of IgG as mediated by the receptor, FcRn: an analysis at the single-molecule level. *Proc. Natl. Acad. Sci. U. S. A.* **101**, 11076–11081 (2004).
 206. Schlothauer, T. *et al.* Analytical FcRn affinity chromatography for functional characterization of monoclonal antibodies. *MAbs* **5**, 576 (2013).
 207. Hermann, H.-J. *Nuklearmedizin: mit 24 Tabellen.* (Elsevier, Urban&FischerVerlag, 2004).
 208. Cherry, S. R., Sorenson, J. A. & Phelps, M. E. *Physics in nuclear medicine e-Book.* (Elsevier Health Sciences, 2012).
 209. Groch, M. W. & Erwin, W. D. SPECT in the year 2000: basic principles. *J. Nucl. Med. Technol.* **28**, 233–244 (2000).
 210. Solon, E. G., Schweitzer, A., Stoeckli, M. & Prideaux, B. Autoradiography, MALDI-MS, and SIMS-MS imaging in pharmaceutical discovery and development. *AAPS J.* **12**, 11–26 (2010).

211. Izumi, N. *et al.* Application of imaging plates to x-ray imaging and spectroscopy in laser plasma experiments (invited). *Rev. Sci. Instrum.* **77**, 10E325 (2006).
212. Iwabuchi, Y., Mori, N., Takahashi, K., Matsuda, T. & Shionoya, S. Mechanism of Photostimulated Luminescence Process in BaFBr:Eu^{2+} Phosphors. *Jpn. J. Appl. Phys.* **33**, 178–185 (1994).
213. Miyahara, J., Takahashi, K., Amemiya, Y., Kamiya, N. & Satow, Y. A new type of X-ray area detector utilizing laser stimulated luminescence. *Nucl. Instruments Methods Phys. Res. Sect. A Accel. Spectrometers, Detect. Assoc. Equip.* **246**, 572–578 (1986).
214. Leblans, P., Vandembroucke, D. & Willems, P. Storage phosphors for medical imaging. *Materials (Basel)*. **4**, 1034–1086 (2011).
215. Fischer, H. A. & Werner, G. *Autoradiography*. (Walter de Gruyter GmbH & Co KG, 1970).
216. Gahan, P. *Autoradiography for biologists*. (Academic Press, 1972).
217. Information, T. Technical Information; Ilford Nuclear Emulsion. 1–6 (2011).
218. Sehlin, D., Fang, X. T., Meier, S. R., Jansson, M. & Syvänen, S. Pharmacokinetics, biodistribution and brain retention of a bispecific antibody-based PET radioligand for imaging of amyloid- β . *Sci. Rep.* **7**, 1–9 (2017).
219. Myrhammar, A. *et al.* Evaluation of an antibody-PNA conjugate as a clearing agent for antibody-based PNA-mediated radionuclide pretargeting. *Sci. Rep.* **10**, (2020).
220. Cheal, S. M. *et al.* An N-Acetylgalactosamino Dendron-Clearing Agent for High-Therapeutic-Index DOTA-Hapten Pretargeted Radioimmunotherapy. **31**, 501–506 (2020).
221. Meyer, J. P. *et al.* Bioorthogonal Masking of Circulating Antibody-TCO Groups Using Tetrazine-Functionalized Dextran Polymers. *Bioconjug. Chem.* **29**, 538–545 (2018).
222. Faresjö, R. *et al.* Brain pharmacokinetics of two BBB penetrating bispecific antibodies of different size. *Fluids Barriers CNS* **18**, 26 (2021).
223. Faresjö, R. *et al.* Transferrin Receptor Binding BBB-Shuttle Facilitates Brain Delivery of Anti-A β -Affibodies. *Pharm. Res.* **39**, 1509–1521 (2022).
224. Gustavsson, T., Syvänen, S., O’callaghan, P. & Sehlin, D. SPECT imaging of distribution and retention of a brain-penetrating bispecific amyloid- β antibody in a mouse model of Alzheimer’s disease. *Transl. Neurodegener.* **9**, 1–11 (2020).
225. Dickinson, B. L. *et al.* Bidirectional FcRn-dependent IgG transport in a polarized human intestinal epithelial cell line. *J. Clin. Invest.* **104**, 903–911 (1999).
226. Ghetie, V. & Ward, E. S. Multiple roles for the major histocompatibility complex class I-related receptor FcRn. *Annu. Rev.*

- Immunol.* **18**, 739–766 (2000).
227. Saxena, A. & Wu, D. Advances in therapeutic Fc engineering - modulation of IgG-associated effector functions and serum half-life. *Front. Immunol.* **7**, 580 (2016).
228. Bern, M. *et al.* An engineered human albumin enhances half-life and transmucosal delivery when fused to protein-based biologics. *Sci. Transl. Med.* **12**, (2020).
229. Roopenian, D. C. *et al.* The MHC class I-like IgG receptor controls perinatal IgG transport, IgG homeostasis, and fate of IgG-Fc-coupled drugs. *J. Immunol.* **170**, 3528–3533 (2003).
230. He, W. *et al.* FcRn-mediated antibody transport across epithelial cells revealed by electron tomography. *Nature* **455**, 542–546 (2008).
231. Vaccaro, C., Zhou, J., Ober, R. J. & Ward, E. S. Engineering the Fc region of immunoglobulin G to modulate in vivo antibody levels. *Nat. Biotechnol.* **23**, 1283–1288 (2005).
232. Swiercz, R. *et al.* Use of Fc-Engineered Antibodies as Clearing Agents to Increase Contrast During PET. *J Nucl Med* **55**, 1204–1207 (2014).
233. Dos Santos, J. B. R., Gomes, R. M. & da Silva, M. R. R. Abdeg technology for the treatment of myasthenia gravis: efgartigimod drug experience. <https://doi.org/10.1080/1744666X.2022.2106972> **18**, 879–888 (2022).
234. Deane, R. *et al.* IgG-assisted age-dependent clearance of Alzheimer’s amyloid beta peptide by the blood-brain barrier neonatal Fc receptor. *J. Neurosci.* **25**, 11495–11503 (2005).
235. Schlachetzki, F., Zhu, C. & Pardridge, W. M. Expression of the neonatal Fc receptor (FcRn) at the blood-brain barrier. *J. Neurochem.* **81**, 203–206 (2002).
236. Cooper, P. R. *et al.* Efflux of monoclonal antibodies from rat brain by neonatal Fc receptor, FcRn. *Brain Res.* **1534**, 13–21 (2013).
237. Zhang, Y. & Pardridge, W. M. Mediated efflux of IgG molecules from brain to blood across the blood-brain barrier. *J. Neuroimmunol.* **114**, 168–172 (2001).
238. Finke, J. M. & Banks, W. A. Modulators of IgG penetration through the blood-brain barrier: Implications for Alzheimer’s disease immunotherapy. *Hum. Antibodies* **25**, 131–146 (2017).
239. Garg, A. & Balthasar, J. P. Investigation of the influence of FcRn on the distribution of IgG to the brain. *AAPS J.* **11**, 553–557 (2009).
240. Chen, N. *et al.* The effect of the neonatal Fc receptor on human IgG biodistribution in mice. *MAbs* **6**, 502 (2014).
241. Arguello, A. *et al.* Molecular architecture determines brain delivery of a transferrin receptor-targeted lysosomal enzyme. *J. Exp. Med.* **219**, (2022).
242. Staudt, M. & Herth, M. M. Clearing and Masking Agents in Pretargeting Strategies. *Pharm. 2023, Vol. 16, Page 497* **16**, 497 (2023).

243. García, M. F. *et al.* 99mTc-bioorthogonal click chemistry reagent for in vivo pretargeted imaging. *Bioorg. Med. Chem.* **24**, 1209 (2016).
244. Shah, M. A. *et al.* Metal-Free Cycloaddition Chemistry Driven Pretargeted Radioimmunotherapy Using α -Particle Radiation. *Bioconjug. Chem.* **28**, 3007–3015 (2017).
245. Lämpchen, T. *et al.* DOTA-tetrazine probes with modified linkers for tumor pretargeting. *Nucl. Med. Biol.* **55**, 19–26 (2017).
246. Membreno, R. *et al.* Towards the Optimization of Click-Mediated Pretargeted Radioimmunotherapy. *Mol. Pharm.* **16**, acs.molpharmaceut.9b00062 (2019).
247. Broek, S. L. van den *et al.* Pretargeted Imaging beyond the Blood Brain Barrier - Utopia or Feasible? *Pharm. 2022, Vol. 15, Page 1191* **15**, 1191 (2022).
248. Lopes van den Broek, S. *et al.* The Alzheimer's disease 5xFAD mouse model is best suited to investigate pretargeted imaging approaches beyond the blood-brain barrier. *Front. Nucl. Med.* **2**, 32 (2022).
249. Bredack, C., Edelmann, M. R., Borroni, E., Gobbi, L. C. & Honer, M. Antibody-Based In Vivo Imaging of Central Nervous System Targets—Evaluation of a Pretargeting Approach Utilizing a TCO-Conjugated Brain Shuttle Antibody and Radiolabeled Tetrazines. *Pharmaceuticals* **15**, 1445 (2022).
250. Rossin, R. *et al.* Highly reactive trans-cyclooctene tags with improved stability for diels-alder chemistry in living systems. *Bioconjug. Chem.* **24**, 1210–1217 (2013).
251. Chang, C.-Y., Chen, J.-Y. & Ke, D.-S. *Essential fatty acids and human brain.* *Acta Neurologica Taiwanica* **18**, (2009).
252. Wager, T. T., Hou, X., Verhoest, P. R. & Villalobos, A. Moving beyond rules: The development of a central nervous system multiparameter optimization (CNS MPO) approach to enable alignment of druglike properties. *ACS Chem. Neurosci.* **1**, 435–449 (2010).
253. Wager, T. T., Hou, X., Verhoest, P. R. & Villalobos, A. Central Nervous System Multiparameter Optimization Desirability: Application in Drug Discovery. *ACS Chem. Neurosci.* **7**, 767–775 (2016).
254. Stéen, J. E. L. *et al.* Lipophilicity and click reactivity determine the performance of bioorthogonal tetrazine tools in pretargeted in vivo chemistry. *ChemRxiv* **4**, 824–833 (2021).
255. Faresjö, R., Sehlin, D. & Syvänen, S. *Age, dose and binding to TfR on blood cells influence brain delivery of a TfR-transported antibody.*
256. Chen, Y. & Xu, Y. Pharmacokinetics of Bispecific Antibody. *Curr. Pharmacol. Reports* **3**, 126–137 (2017).
257. Morrison, J. I., Metzendorf, N. G., Rofo, F., Petrovic, A. & Hultqvist, G. A single chain fragment constant (scFc) design enables easy production of a monovalent BBB transporter and provides an improved

- brain uptake at elevated doses. *J. Neurochem.* (2023). doi:10.1111/JNC.15768
258. Haqqani, A. S. *et al.* Intracellular sorting and transcytosis of the rat transferrin receptor antibody OX26 across the blood-brain barrier in vitro is dependent on its binding affinity. *J. Neurochem.* **146**, 735–752 (2018).
259. Johnsen, K. B., Burkhart, A., Thomsen, L. B., Andresen, T. L. & Moos, T. Targeting the transferrin receptor for brain drug delivery. *Prog. Neurobiol.* **181**, 101665 (2019).
260. Verel, I. *et al.* Long-lived positron emitters zirconium-89 and iodine-124 for scouting of therapeutic radioimmunoconjugates with PET. *Cancer Biother. Radiopharm.* **18**, 655–661 (2003).
261. Deri, M. A., Zeglis, B. M., Francesconi, L. C. & Lewis, J. S. PET imaging with ⁸⁹Zr: from radiochemistry to the clinic. *Nucl. Med. Biol.* **40**, 3–14 (2013).
262. Fissers, J. *et al.* Synthesis and Evaluation of a Zr-89-Labeled Monoclonal Antibody for Immuno-PET Imaging of Amyloid-β Deposition in the Brain. *Mol. imaging Biol.* **18**, 598–605 (2016).
263. Gustafsson, S. *et al.* Blood-brain barrier integrity in a mouse model of Alzheimer’s disease with or without acute 3D6 immunotherapy. *Neuropharmacology* **143**, 1–9 (2018).
264. De Rosa, L., Di Stasi, R., Romanelli, A. & D’andrea, L. D. Exploiting Protein N-Terminus for Site-Specific Bioconjugation. *Mol. 2021, Vol. 26, Page 3521* **26**, 3521 (2021).
265. Waibel, R. *et al.* Stable one-step technetium-99m labeling of His-tagged recombinant proteins with a novel Tc(I)-carbonyl complex. *Nat. Biotechnol.* **17**, 897–901 (1999).
266. Guimaraes, C. P. *et al.* Site-specific C-terminal and internal loop labeling of proteins using sortase-mediated reactions. *Nat. Protoc.* **8**, 1787–1799 (2013).

Acta Universitatis Upsaliensis

*Digital Comprehensive Summaries of Uppsala Dissertations
from the Faculty of Medicine 1927*

Editor: The Dean of the Faculty of Medicine

A doctoral dissertation from the Faculty of Medicine, Uppsala University, is usually a summary of a number of papers. A few copies of the complete dissertation are kept at major Swedish research libraries, while the summary alone is distributed internationally through the series Digital Comprehensive Summaries of Uppsala Dissertations from the Faculty of Medicine. (Prior to January, 2005, the series was published under the title “Comprehensive Summaries of Uppsala Dissertations from the Faculty of Medicine”.)

Distribution: publications.uu.se
urn:nbn:se:uu:diva-499059



ACTA
UNIVERSITATIS
UPSALIENSIS
UPPSALA
2023